Chemoreceptive Neuron MOS (CυMOS) Transistors for Environmental Monitoring:

Detection in Fluid and Gas Ambients with Field Programmability and High Reliability

Edwin C. Kan

School of Electrical and Computer Engineering
Cornell University

CORNELL

This research is funded by
U.S. EPA - Science To Achieve Results (STAR) Program
Grant # RD83

Motivation

- Silicon-based autonomous microsystem
  - **Sensing ability**
  - Communication
  - Computation
  - Control/memory units
  - **Actuation capability**
  - Power self-sufficient
  - Ease of manufacture

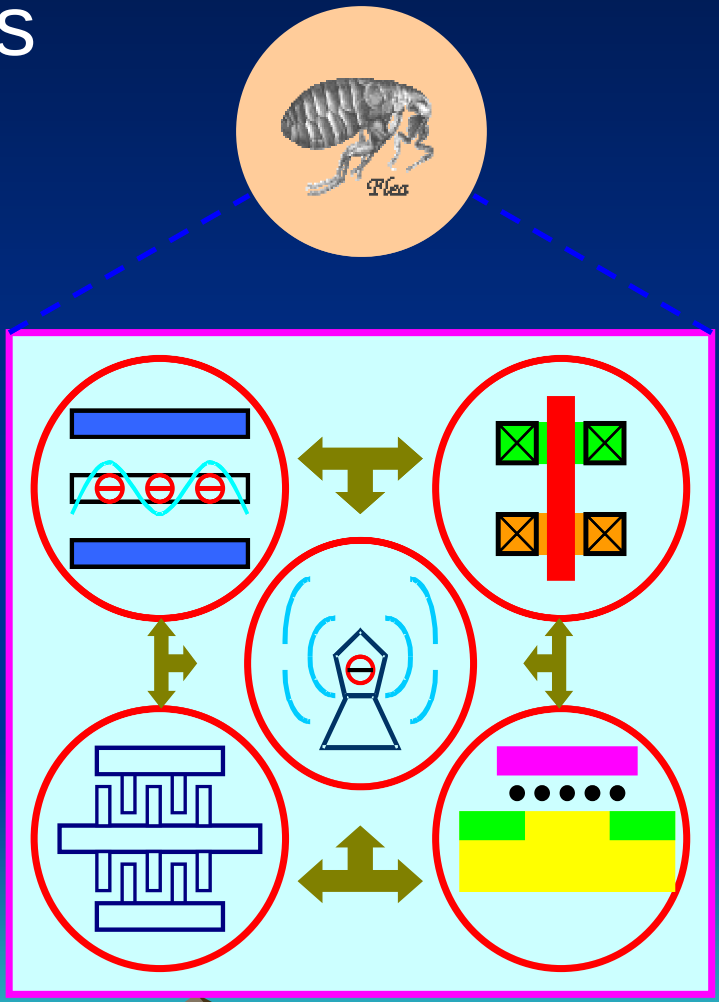

CORNELL

Outline

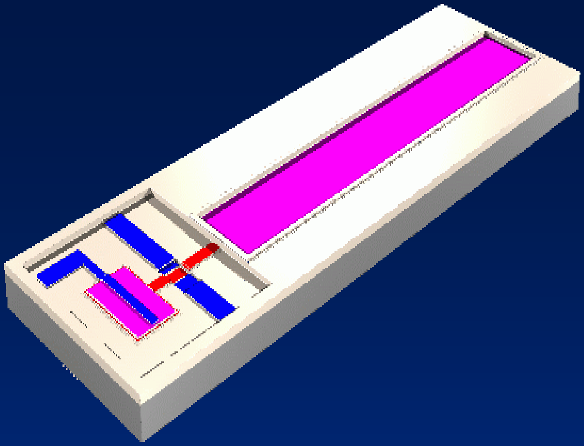

- CυMOS Overview
  - Why – Review of literature
  - What – CυMOS device structure
  - How – Device operation
    - Sensors
      - Fluid ambient (Na^+, K^+ , Ca^{2+}, BSA and SDS)
      - Gas ambient (CO_2)
      - Readout circuits
    - Actuators
  - Conclusion

CORNELL

Literature Review (1/3)

- FET-based (Bergveld 1970)
  - Materials in contact with silicon oxide
  - pH sensitive
  - Many spin-offs
    - ChemFET
    - ENFET (Enzyme)
    - IMMUNOFET

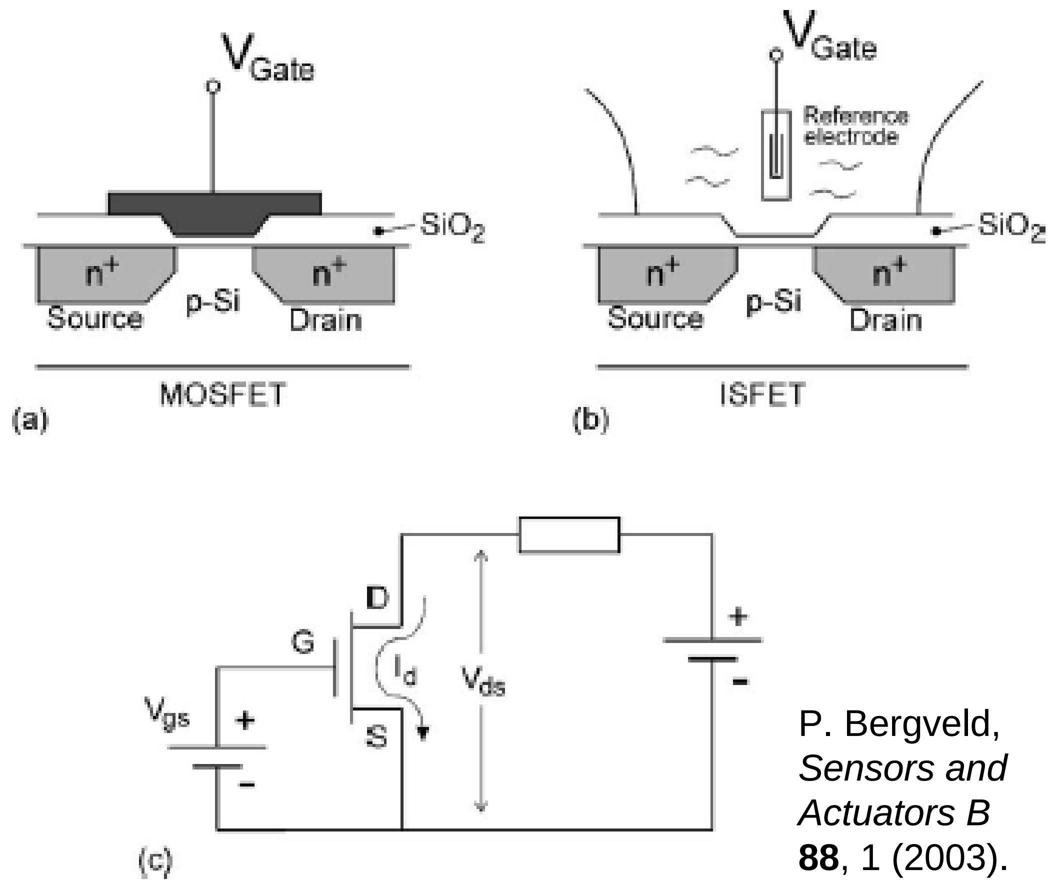

P. Bergveld, *Sensors and Actuators B* **88**, 1 (2003).

Literature Review (2/3)

Resistive-based

- Tune resistivity in the sensing scheme
- Gardner (1991)
- Lewis (1996): electronic nose
- Advantage: sensitivity from tunneling distance modulation

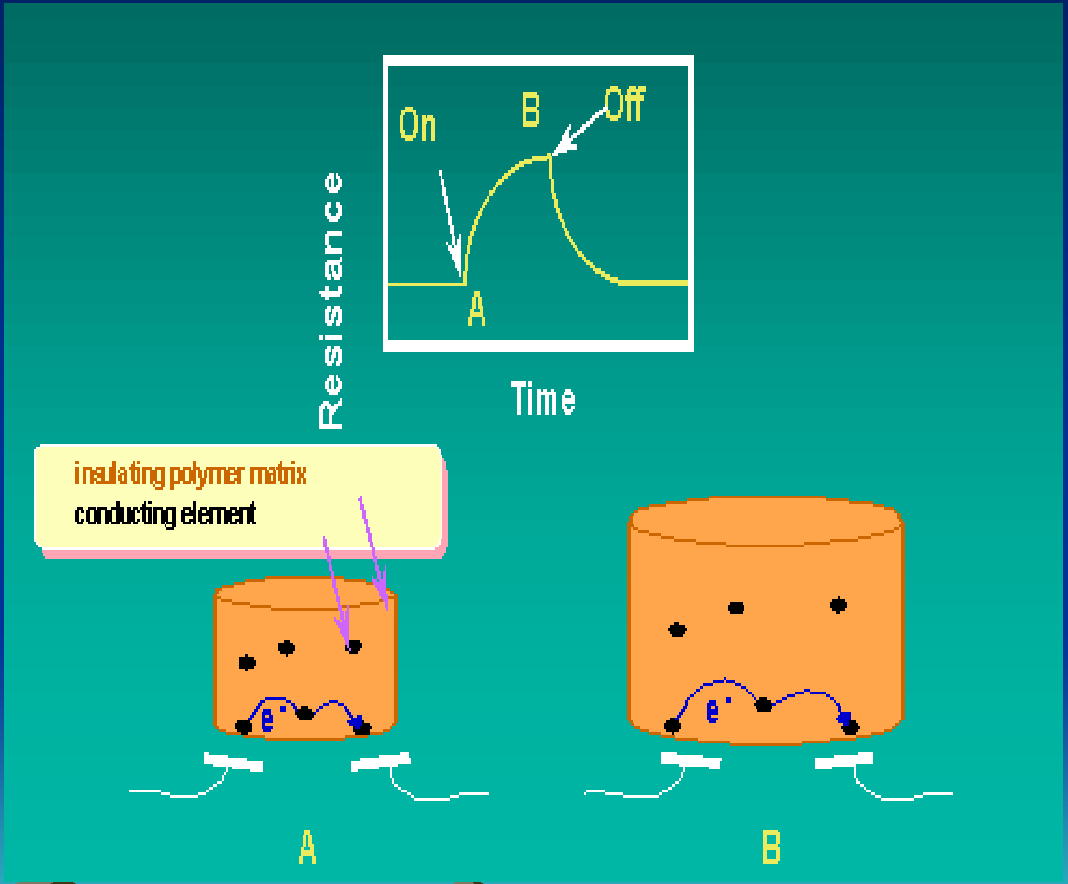

CORNELL

Literature Review (3/3)

- Chemicapacitive
  - Yamamoto (1987)
  - Steiner (1995)
- Chemomechanical
  - Grimshaw (1990)
  - Lang (1999)

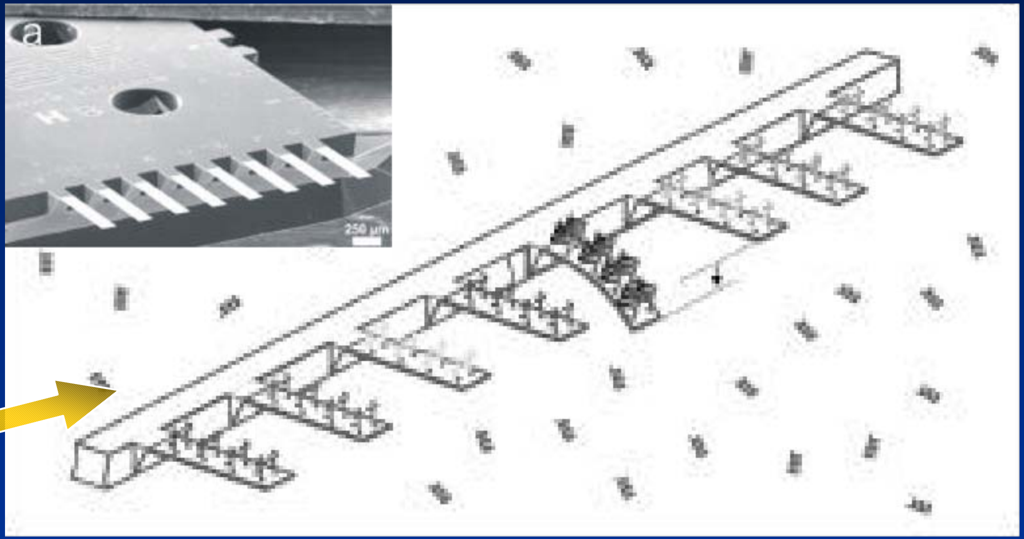

- SAW-IDT (Inter-Digital Transducers)
  - Wenzel (1990)
  - Nakamoto (1991)

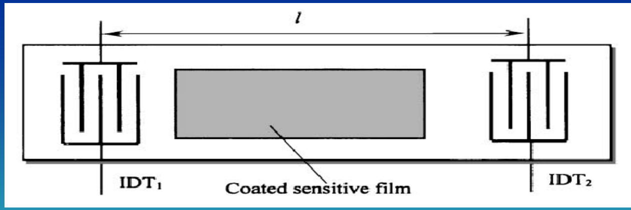

Dong, et al., *Sensors and Actuators* **B76**, 130 (2001).

CORNELL

Why CυMOS?

- Integrated device structure for sensors
- Enhancement of DOFs in sensing
- Ease of integration with current CMOS technology
- Charge-based operation to reduce power consumption
- Potential for sensor-array application
- Possibility to integrated sensors and actuators with the same structure

CORNELL

CυMOS Objectives

- High sensitivity
- High selectivity
- Reproducibility, stability and reliability
- Simple calibration and reset protocols
- Field reconfigurability
- Versatile transient measurement
- Low power consumption in the system
- Low manufacturing cost

CυMOS Device Structure

- Extended floating gate

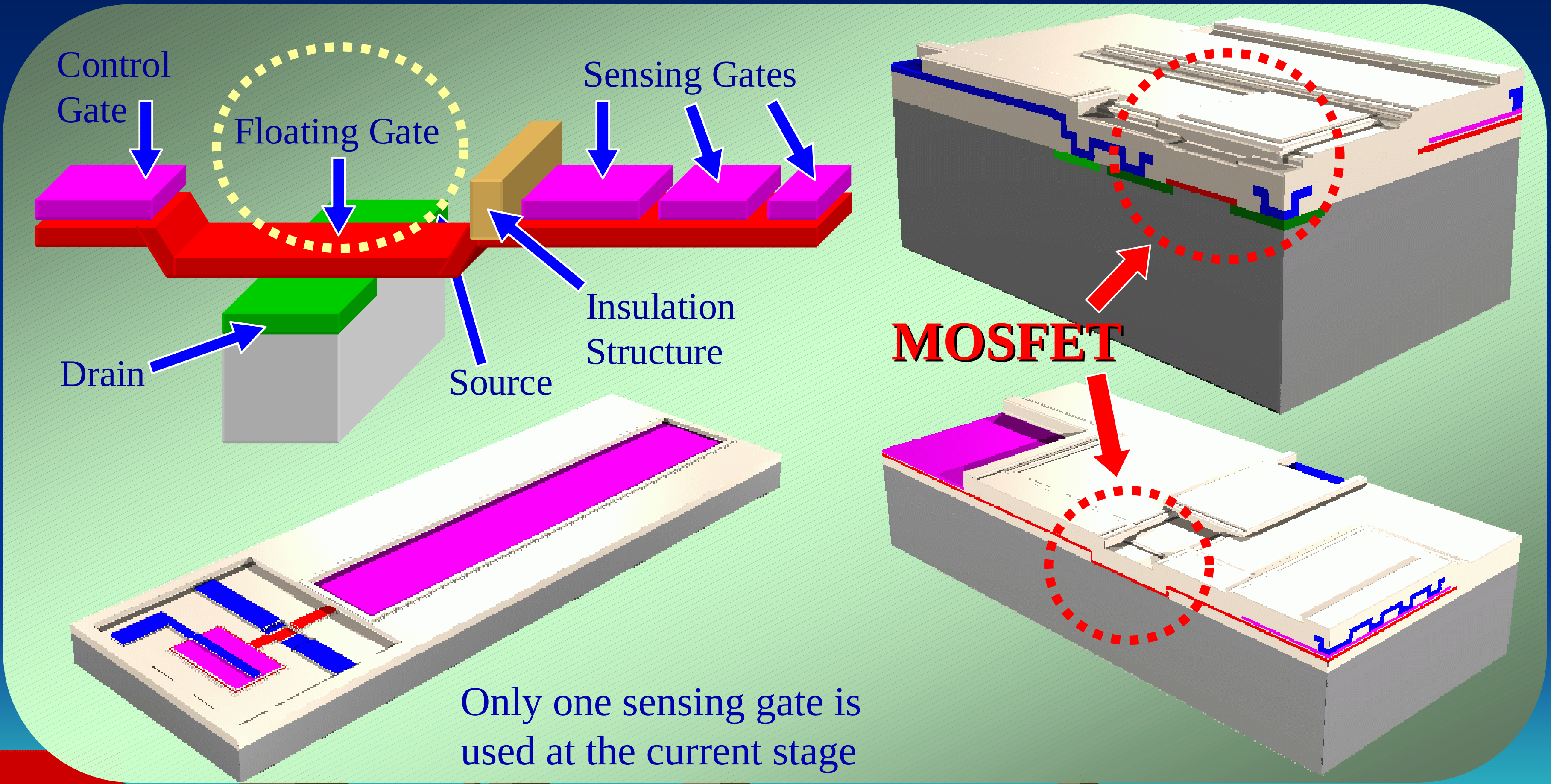

CORNELL

Polymer-Coating Parameters

Polymer Coating	**Solution**	**Molecular Weight**
poly(vinyl acetate)	20 mg in 10 mL Tetrahydrofuran	90,000
poly(vinyl butyral)	20 mg in 10 mL Tetrahydrofuran	100,000–150,000
poly(ethylene -co- vinyl acetate)	100 mg in 10 mL Benzene	72:28 (wt.)
poly(vinyl chloride)	20 mg in 10 mL Tetrahydrofuran	110,000

Polymer Coating	**Thickness (nm)**	**Roughness Ra (nm)**	**Roughness Rq (nm)**
poly(vinyl acetate)	50	64	88
poly(vinyl butyral)	25	20	27
poly(ethylene -co- vinyl acetate)	30	2	2
poly(vinyl chloride)	30	8	13

CORNELL

Dip-Pen Technology

- For smaller sensing gates

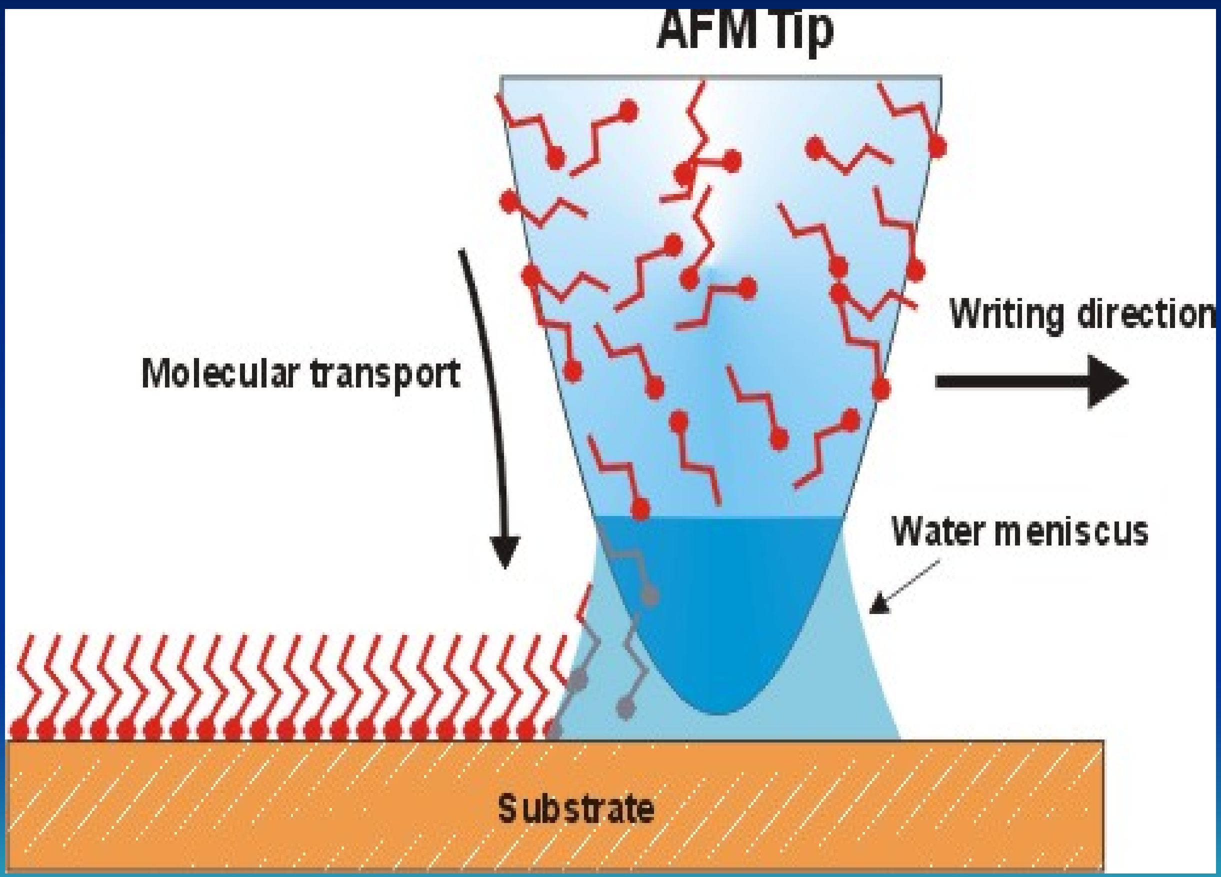

- Molecules delivered from the AFM tip to solid substrate via capillary transport
- 30-nm linewidth resolution

D. Piner, J. Zhu, F. Xu, and S. Hong, C. A. Mirkin, *Science* **283**, 661 (1999).

CORNELL

Microfluidic Channels

- Close-up views

Outline

- Development of the chemoreceptive neuron MOS (CνMOS) trasistors
  - **Device operations and results**
    - **Sensors**
    - Actuators

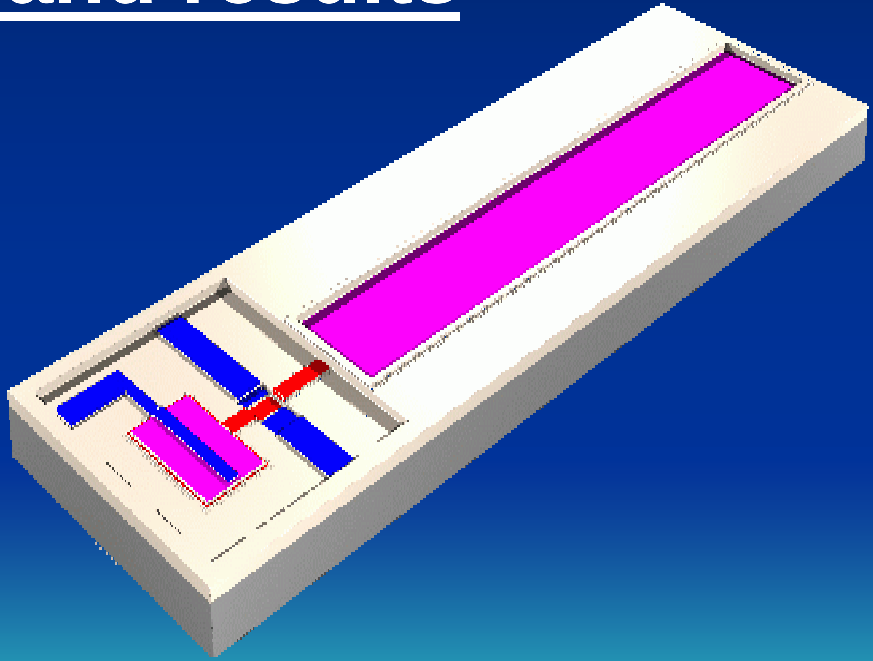

Device Operation

- Record initial device *I*-*V* characteristics
- Apply polymer coating and insulation elastomer
- Deliver fluid to the microfluidic channel (base buffer, electrolytes, or buffer loaded with protein molecules)
- Observe and record changes in threshold voltages (V_t) and subthreshold slopes (*S*): extract C_{SG} *and* ϕ_{OHP}
- *Electron-tunneling operation: apply bias (30V or -30V for 50 seconds) at the control gate*
- Observe and record V_t and *S*
- Perform cleansing steps (e.g. rinsing, N_2 drying)
- Re-align insulation layer and repeat *I*-*V* measurements

CORNELL

Phenomena at the Interface

- GCS model

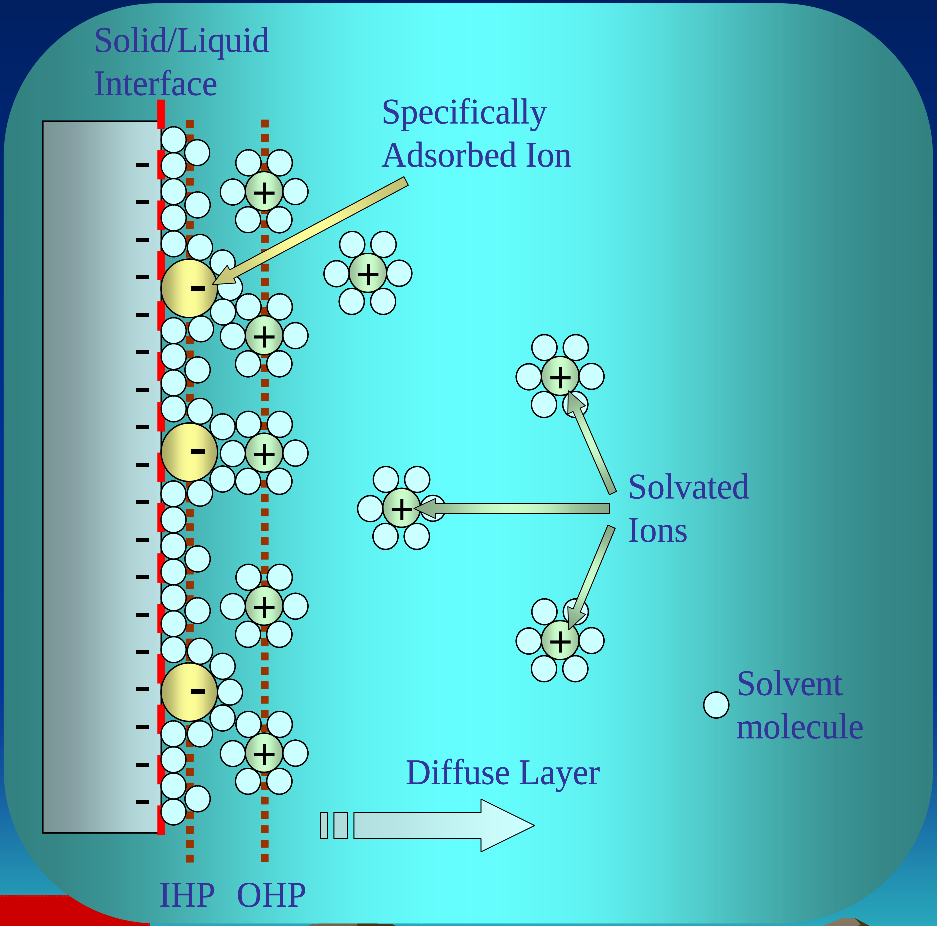

Double-layer capacitance

$$\frac{1}{C_{EDL}} = \frac{1}{C_H} + \frac{1}{C_{DIF}}$$

C_H: Helmholtz-plane capacitance

$$C_H = \int_0^{A_{SG}} \left(\frac{\varepsilon_r \varepsilon_0}{x_{OHP}} \right) dA$$

x_{OHP}: dist. between Helmholtz planes

C_{DIF}: Diffuse-layer capacitance

$$C_{DIF} = \int_0^{A_{SG}} \left(\frac{2\varepsilon_r \varepsilon_0 z^2 q^2 n}{kT} \right)^{1/2} \cosh\left(\frac{zq\phi_{OHP}}{2kT} \right) dA$$

z: magnitude of the charge on the ions
n: concentration of the ions
ϕ_{OHP}: potential at the OHP

CORNELL

Capacitive-Divider Model

$$I = I_0 e^{\kappa V_{FG}/U_T}\left(e^{-V_S/U_T} - e^{-V_D/U_T}\right)$$

Slope

$$\kappa = C_{ox}/(C_{ox} + C_{dep})$$

Subthreshold current model

$$\Delta V_T = -\frac{Q}{C_T} - \frac{C_{gs}}{C_T}V_S - \frac{C_{gd}}{C_T}V_D$$

Above-threshold voltage-shift model

$$V_{FG} = \frac{Q}{C_T} + \frac{C_{gs}}{C_T}V_S + \frac{C_{gd}}{C_T}V_D + \frac{C_{CG}}{C_T}V_{CG} + \frac{C_{SG}}{C_T}V_{SG}$$

$$C_T = (C_{ox} // C_{dep}) + C_b + C_{gs} + C_{gd} + C_{CG} + C_{SG}$$

Changed by fluids

Sample IV Illustration

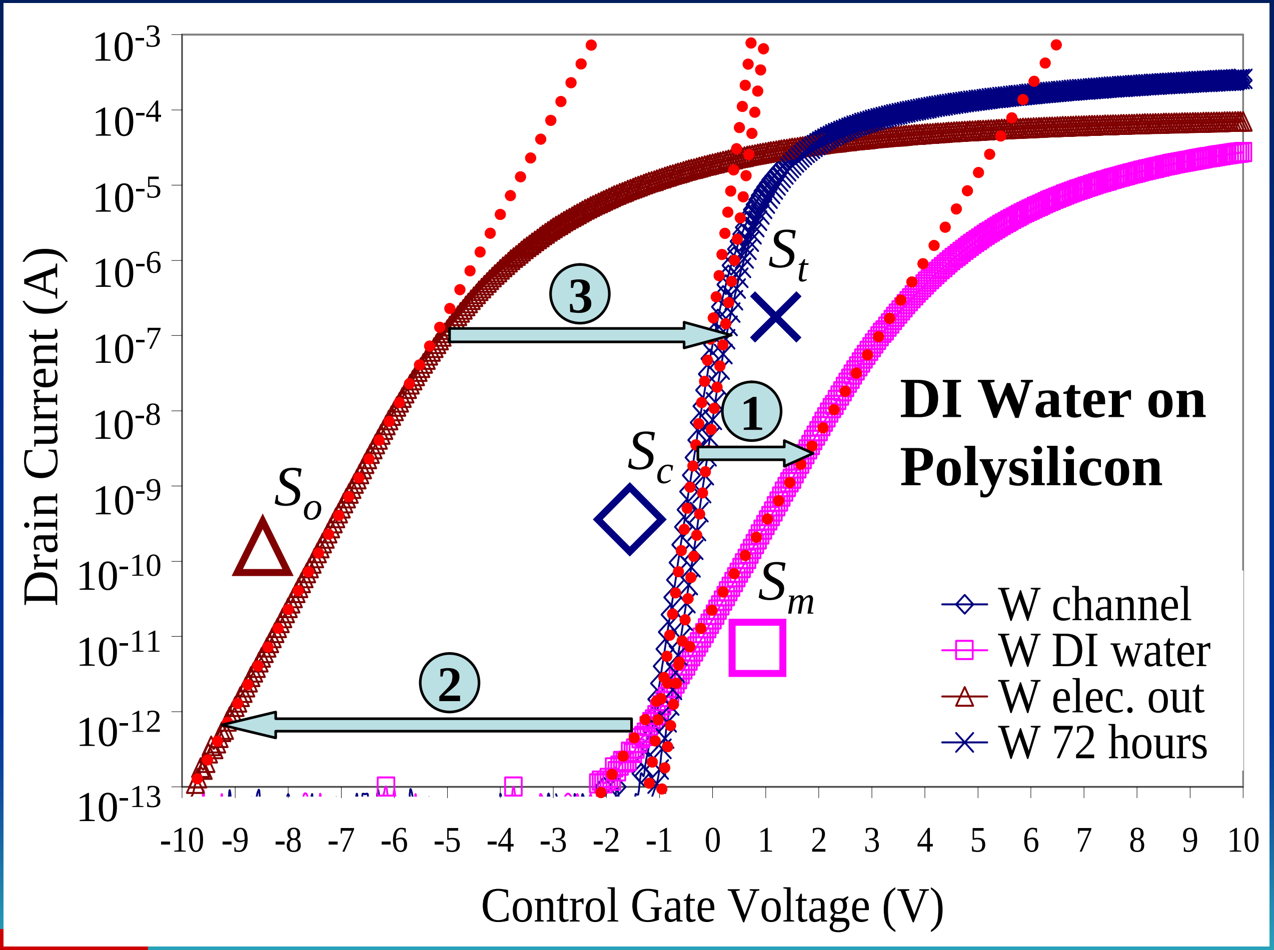

Notations:

c : after applying insulation elastomer with microfluidic channels

m : after delivering the sample fluid

o : after tunneling electrons out of the floating gate

t : after cleansing steps and a period of time in the dry box with constant N_2 flow

CORNELL

Sensing-Gate Responses

- Influence from the fluid
  - Induce image charge at the extended floating gate
  - Modify series capacitance to the sensing gate
  - Affect floating-gate potential and total capacitive load; create distinctive threshold-voltage shifts and subthreshold-slope variations
- Capacitance indication
  - Collect information via capacitive coupling from the fluid bulk to the extended floating-gate structure
  - Detect variations before and after electron-tunneling operations

Subthreshold Slopes

$$C_T = (C_{ox} // C_{dep}) + C_b + C_{gs} + C_{gd} + C_{CG} + C_{SG}$$

$$V_{FG} = \frac{Q}{C_T} + \frac{C_{gs}}{C_T}V_S + \frac{C_{gd}}{C_T}V_D + \frac{C_{CG}}{C_T}V_{CG} + \frac{C_{SG}}{C_T}V_{SG}$$

$$I = I_0 e^{\kappa V_{FG}/U_T}(e^{-V_S/U_T} - e^{-V_D/U_T})$$

$$S \equiv \left[\frac{\partial(\log_{10} I)}{\partial V_{CG}}\right]^{-1}$$

$$S = \frac{U_T \ln 10}{\kappa}\left(\frac{C_T}{C_{CG}}\right)$$

Extraction of *S* values

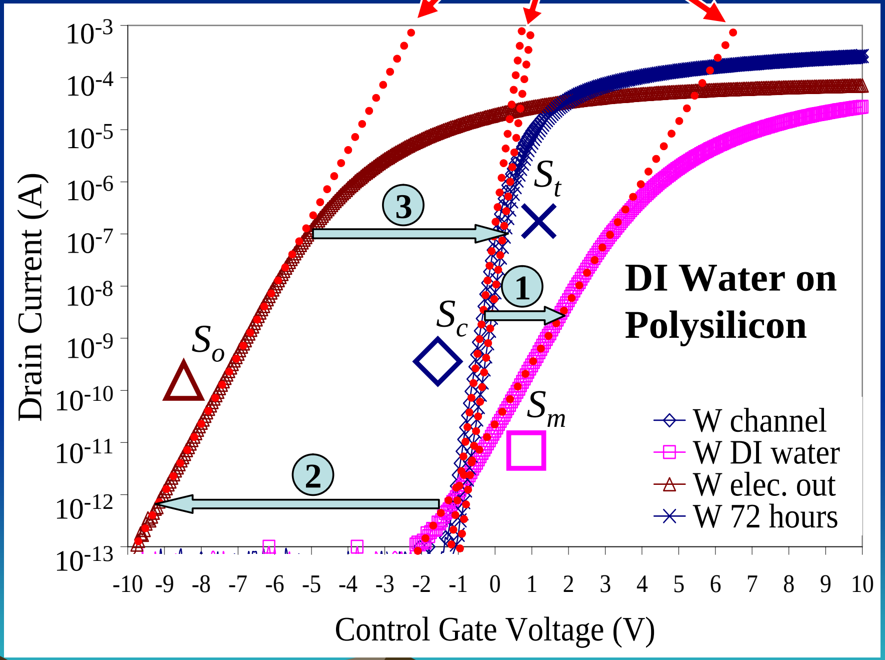

CORNELL

Data Analyses

- Extraction of subthreshold slopes from the measured *I-V* recordings
- Direct estimation of sensing-gate capacitance (C_{SG}), eliminating control-gate capacitance (C_{CG}) variation

$$C_T = (\beta S)\ C_{CG}$$

$$C_T = C_p + C_{CG} + C_{SG}$$

$$C_{SG} = \left(\frac{\beta S - 1}{\beta S_r - 1}\right)\left(C_{SGr} + C_{pr}\right) - C_p$$

$$C_p = (C_{ox} // C_{dep}) + C_b + C_{gs} + C_{gd}$$

$$\beta = \kappa / \left(U_T \ln 10\right)$$

CORNELL

Reference S_r

5 mM KCl	$d1_r$	$d1_c$	$d1_m$	$d1_i$	$d1_t$	$d2_r$	$d2_c$	$d2_m$	$d2_i$	$d2_t$
polysilicon	**148**	177	553	728	166	**200**	213	771	1019	217
poly(vinyl acetate)	**187**	198	270	272	194	**284**	296	435	455	293
poly(vinyl butyral)	**228**	231	687	985	228	**160**	176	663	830	165
poly(ethylene -co-vinyl acetate)	**163**	197	673	711	180	**156**	183	575	668	166
poly(vinyl chloride)	**288**	301	469	491	279	**212**	215	1164	1308	219

Notations:

d1, d2 : device 1, device 2

r : initial reference

c : after channel formation

m : after fluid delivery

Normalization required to get rid of the fabrication variation

i : electron tunneling in, 30 V, 50 s.

t : recordings after cleansing steps and a period of time in the dry box

CORNELL

Normalized ΔC_{SG}

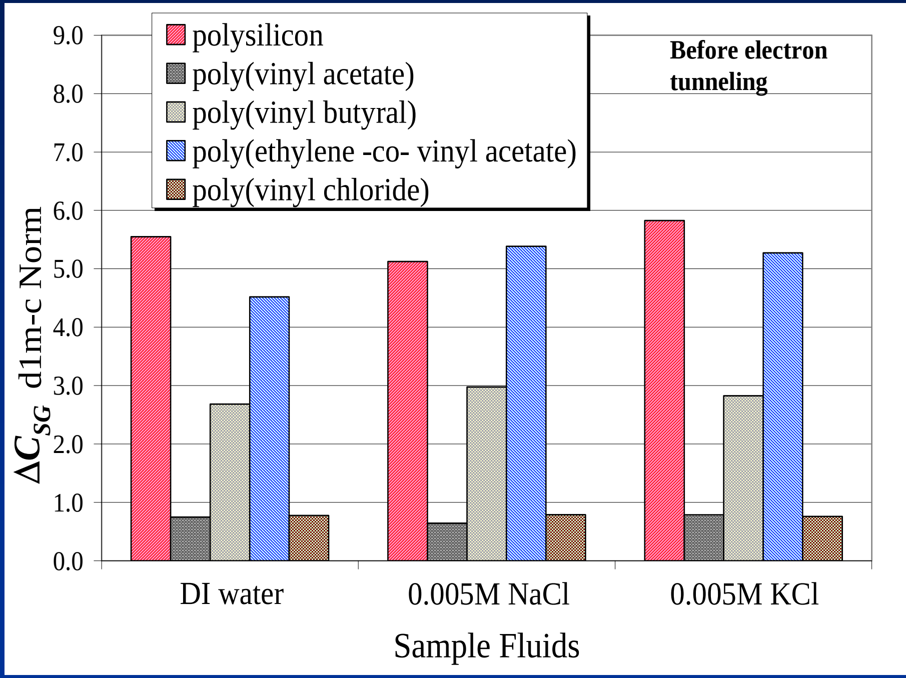

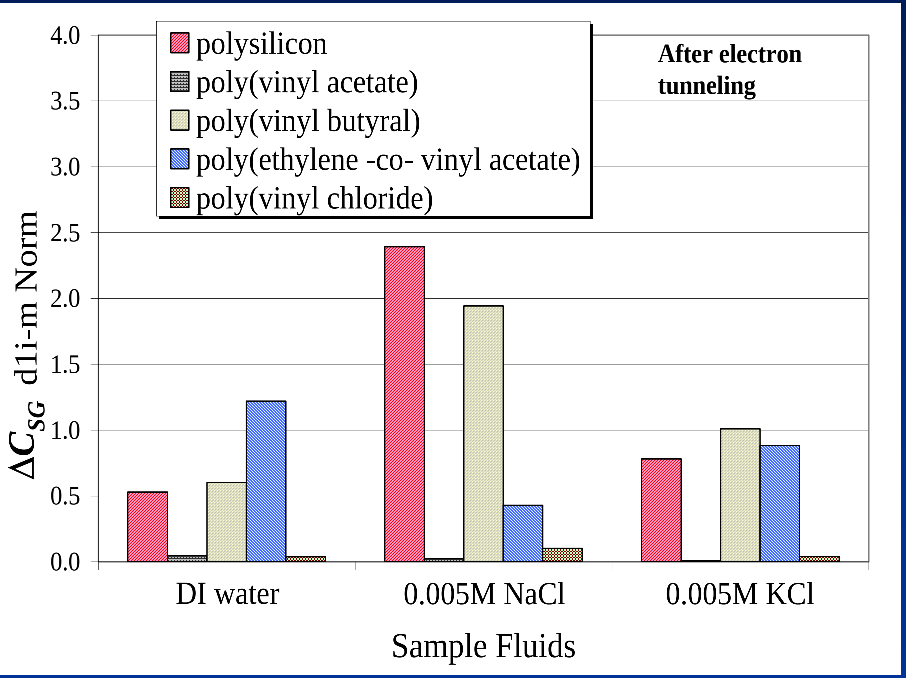

Before electron injection

<u>Variation by polymers</u> (√)

<u>Difference between fluids</u> (X)

After electron injection

<u>"Discernible patterns"</u>

CORNELL

Selectivity Demonstration (1/2)

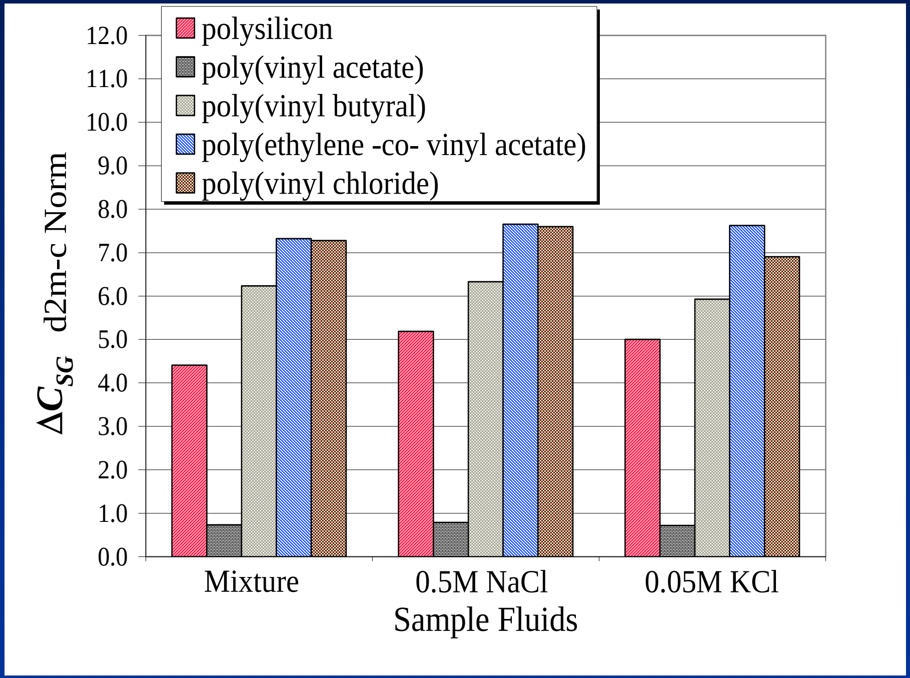

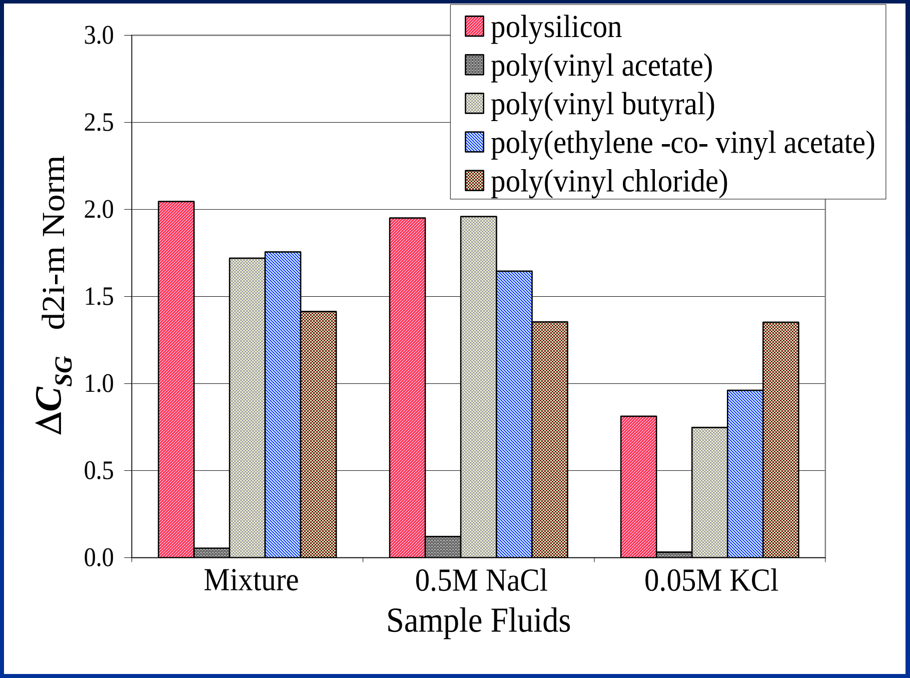

Mixture contains both solutions in corresponding concentration

Before electron injection

"Difference not obvious"

After electron injection

"Discernible patterns"

CORNELL

Selectivity Demonstration (2/2)

- Sensor-array plots

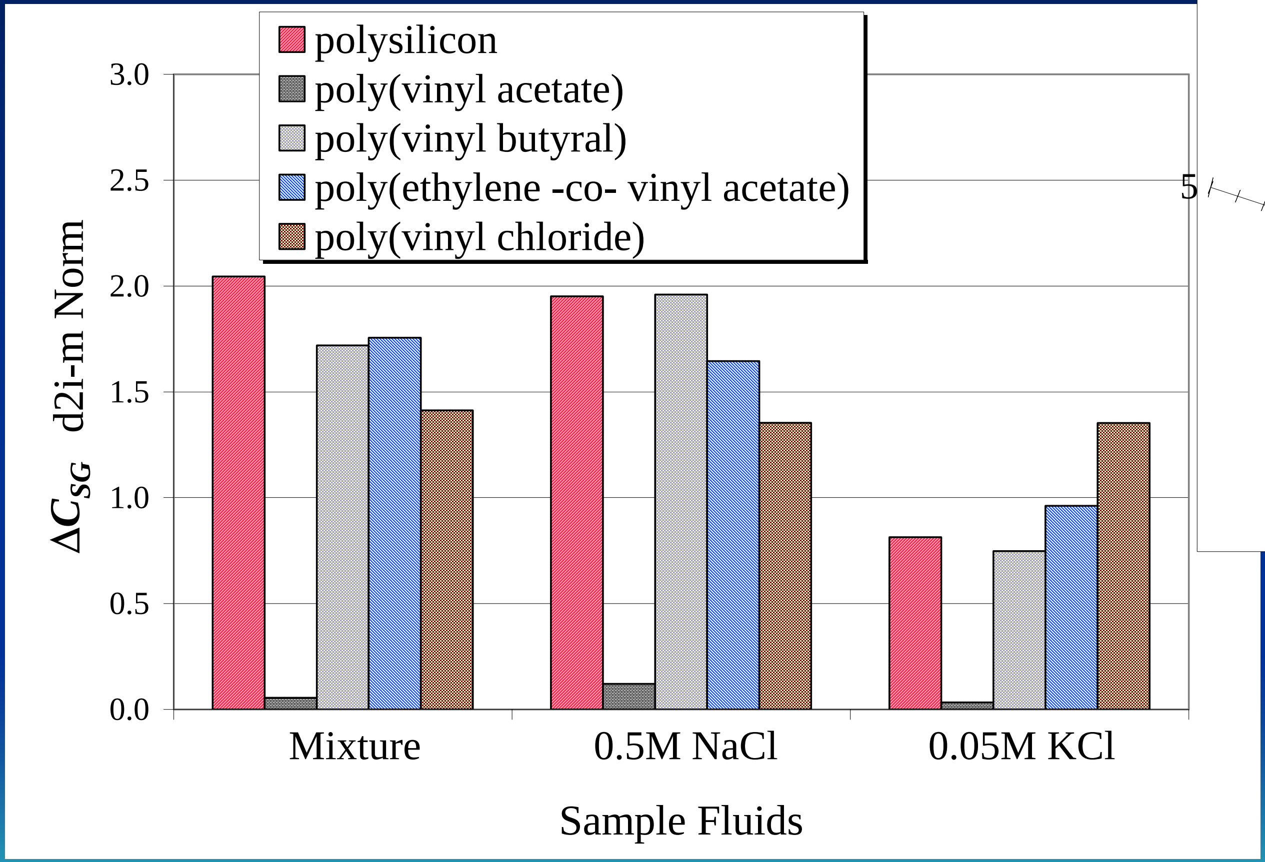

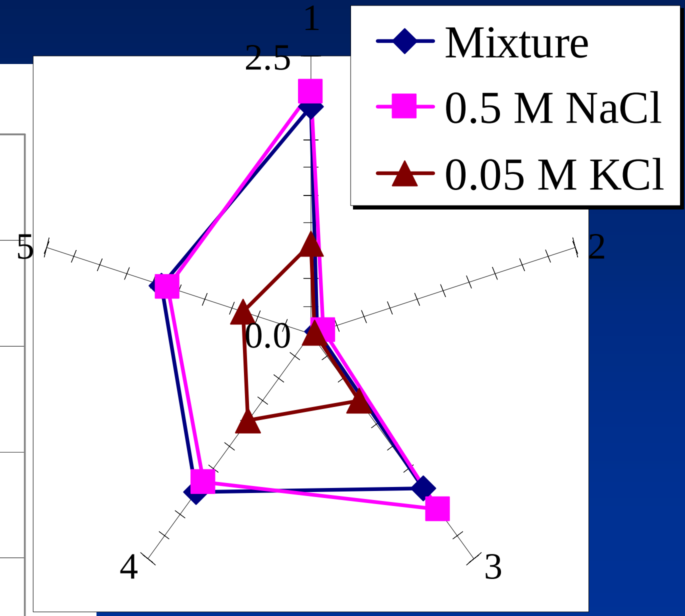

- Additive or subtractive responses in the sensor-array plots

Double-Layer Parameters (1/3)

- ΔC_{dif} from extracted S

ΔC_{dif} ($\mu F/cm^2$)	DI Water	NaCl Solution				KCl Solution			
		50μM	0.005M	0.05M	0.5M	50μM	0.005M	0.05M	0.5M
polysilicon	6.4	7.0	7.5	19.3	26.0	5.7	4.9	4.0	4.0
poly(vinyl acetate)	***20.1***	1.7	7.5	8.3	114.5	6.6	7.6	74.6	***15.0***
poly(vinyl butyral)	1.8	6.0	13.2	16.4	33.6	4.8	4.3	3.3	***4.0***
poly(ethylene -co-vinyl acetate)	1.2	8.9	67.7	105.1	***9.9***	***9.0***	0.9	1.3	2.3
poly(vinyl chloride)	1.1	2.1	3.2	8.3	20.6	0.4	2.4	26.6	***14.9***

$$S = \frac{U_T \ln 10}{\kappa}\left(\frac{C_T}{C_{CG}}\right)$$

$$C_{SG} = \left(\frac{\beta S - 1}{\beta S_r - 1}\right)\left(C_{SGr} + C_{pr}\right) - C_p$$

$$\beta = \frac{\kappa}{U_T \ln 10}$$

Double-Layer Parameters (2/3)

- Extracted ϕ_{OHP} (before elec. injection)

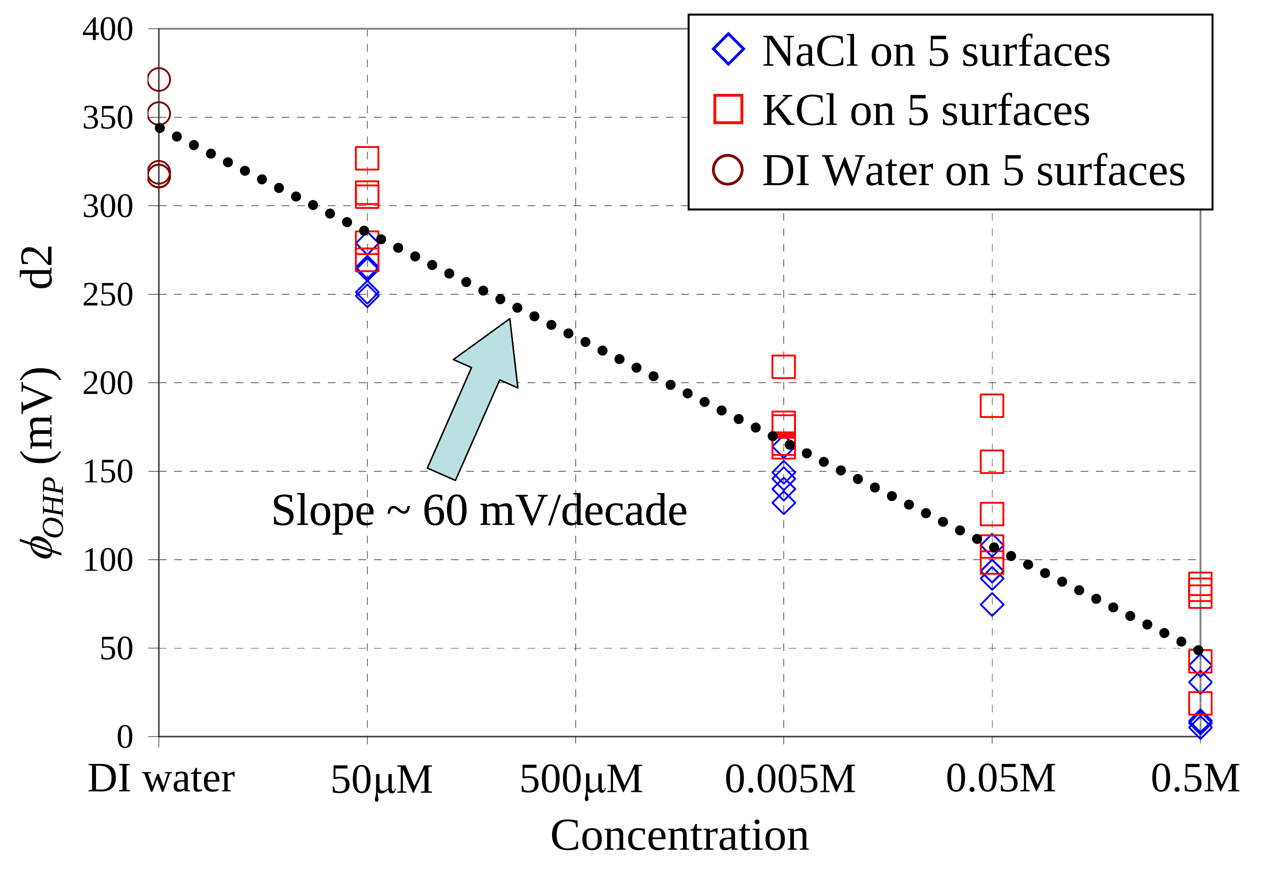

- Nernst Equation

$$E = E_0 + \frac{RT}{nF}\ln\left(\frac{C_{Ox}}{C_{Rd}}\right)$$

$$Ox + ne \Leftrightarrow Rd$$

- *RT/F = kT/q* ~ 25.9 mV at room temp.
- ϕ_{OHP} decreases at ~ 60 mV/dec. with increases in concentration

CORNELL

Double-Layer Parameters (3/3)

- $\Delta\phi_{OHP}$ (after electron injection)

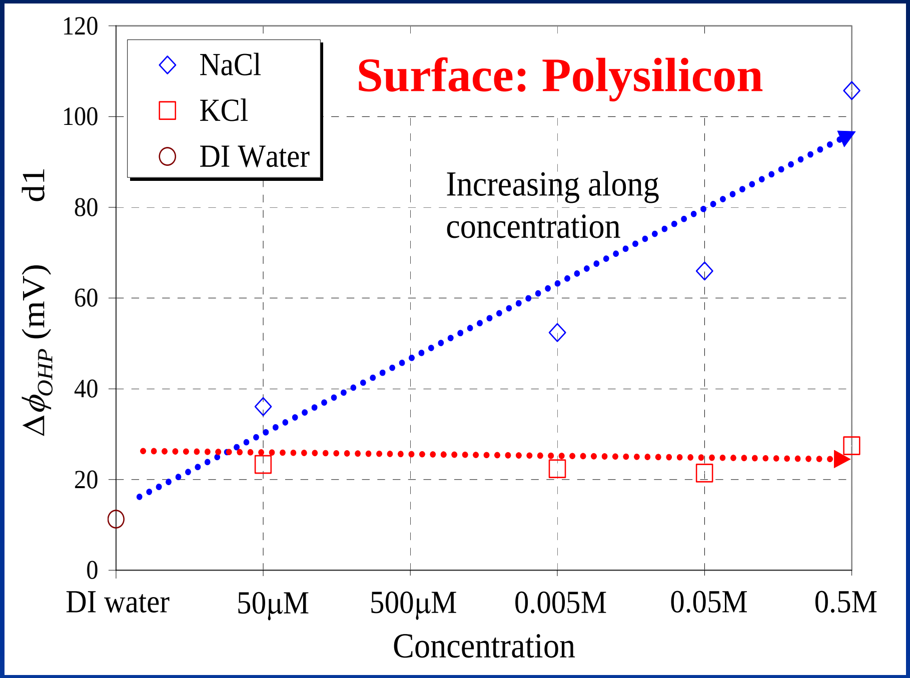

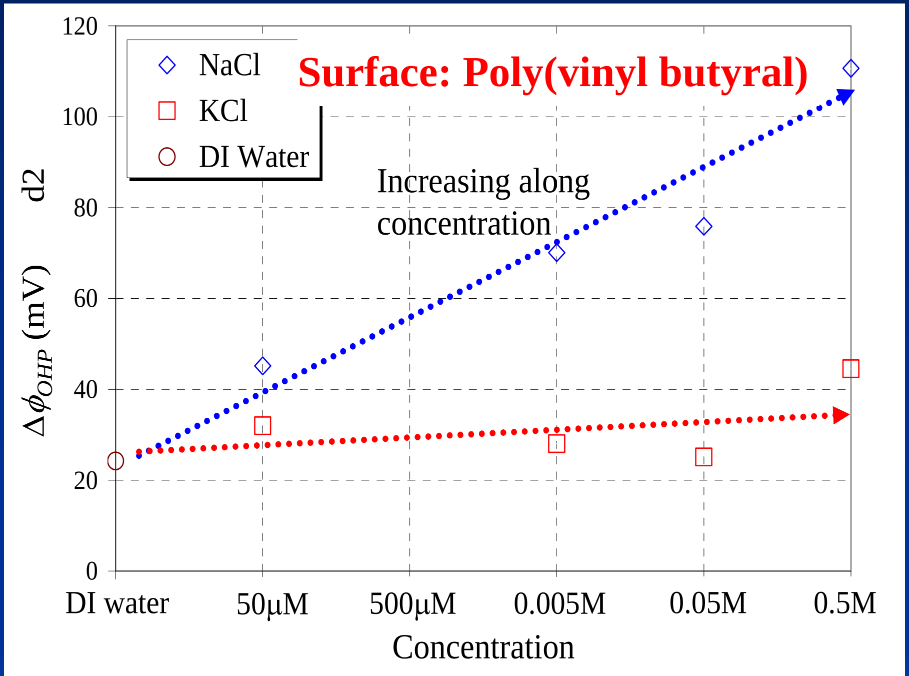

The change of the ϕ_{OHP} increases with increasing concentration in NaCl

For KCl solution, no significant increasing trend is observed as in NaCl

CORNELL

Detection in Gas Ambients

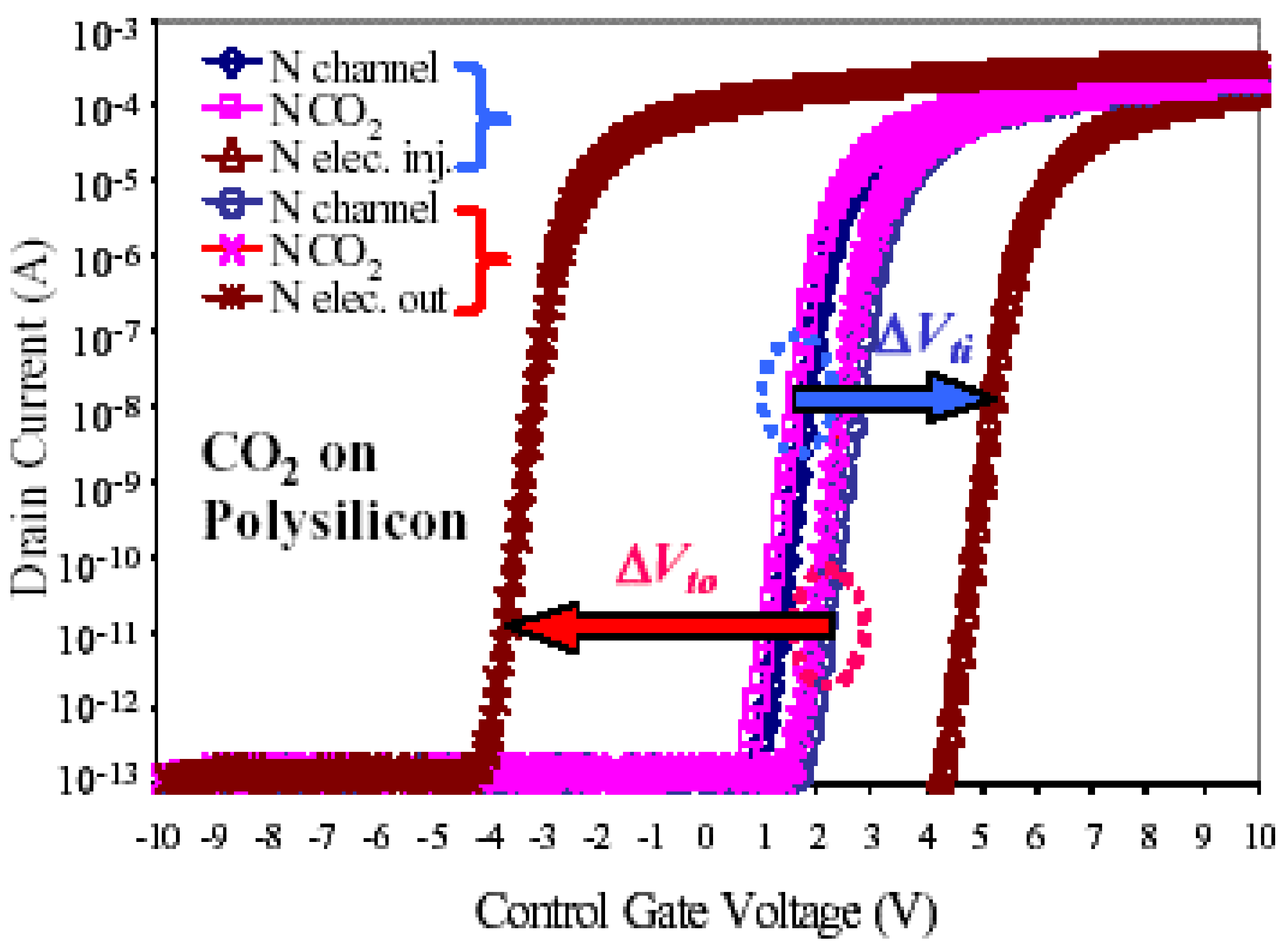

CORNELL

Protein Sensing

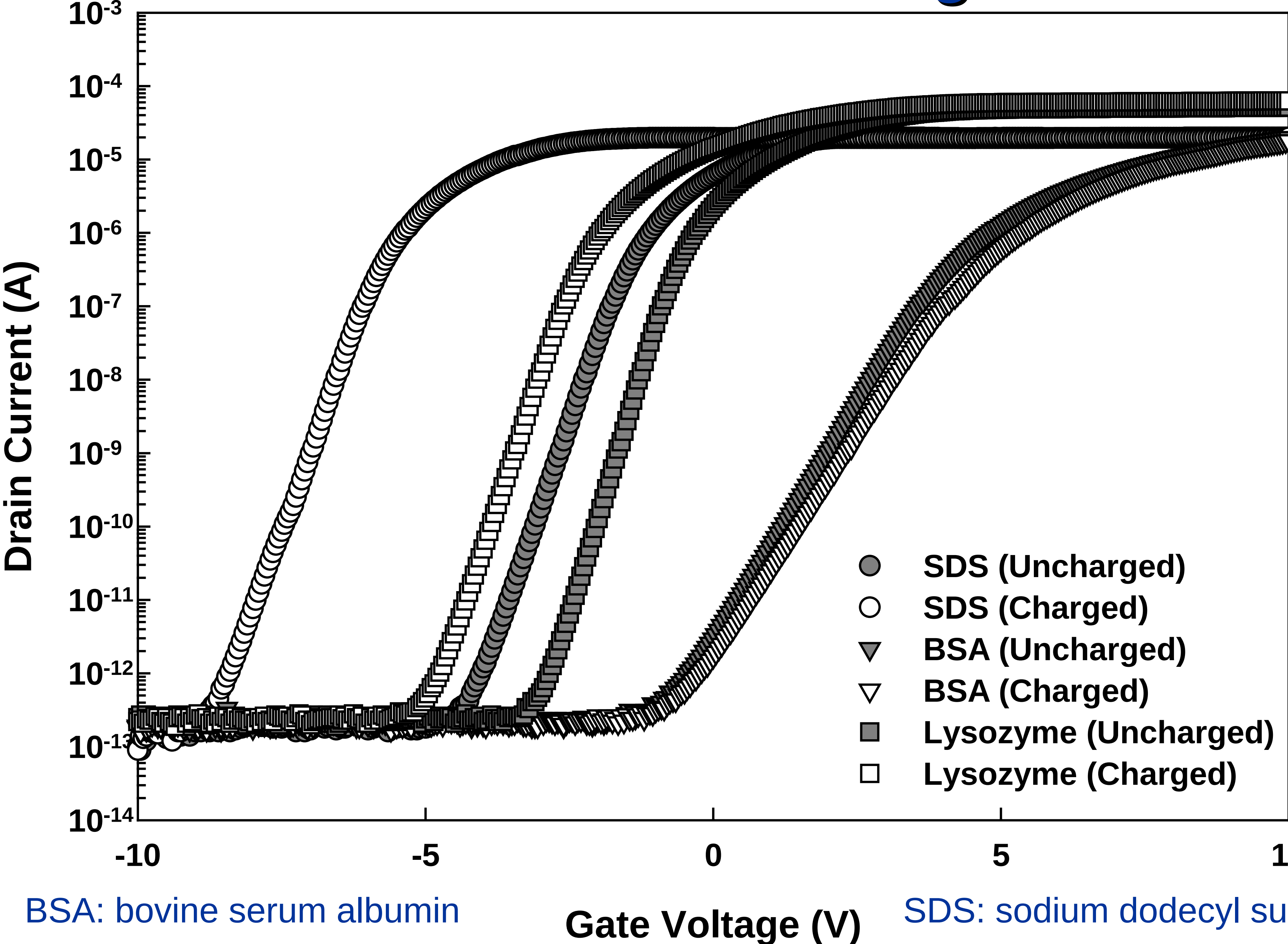

BSA: bovine serum albumin

SDS: sodium dodecyl sulfate

CMOS Circuit Integration

$$\Delta V_{\mathrm{d}} = \frac{2U_{\mathrm{T}}}{\kappa}\frac{C_{\mathrm{T}}}{C_{\mathrm{CG1}}} ln\left(\frac{e^{\sqrt{I_{\mathrm{in}}^{\mathrm{H}}/I_{\mathrm{s}}}}-1}{e^{\sqrt{I_{\mathrm{in}}^{\mathrm{L}}/I_{\mathrm{s}}}}-1}\right)$$

$$\propto S\left(=\frac{ln10U_{\mathrm{T}}}{\kappa}\frac{C_{\mathrm{T}}}{C_{\mathrm{CG1}}}\right)$$

MOSIS AMI foundry fabrication (April 2004)

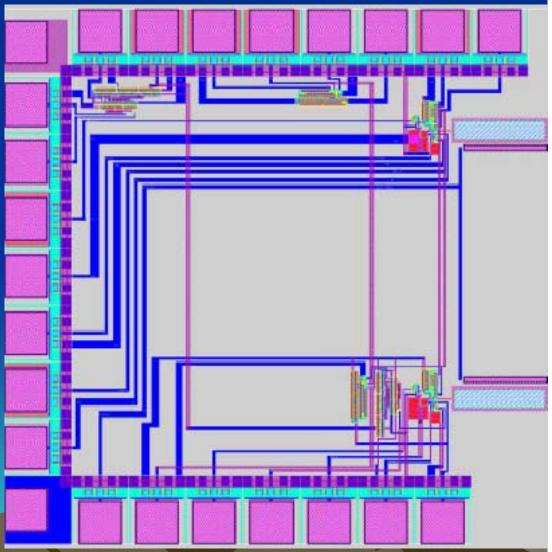

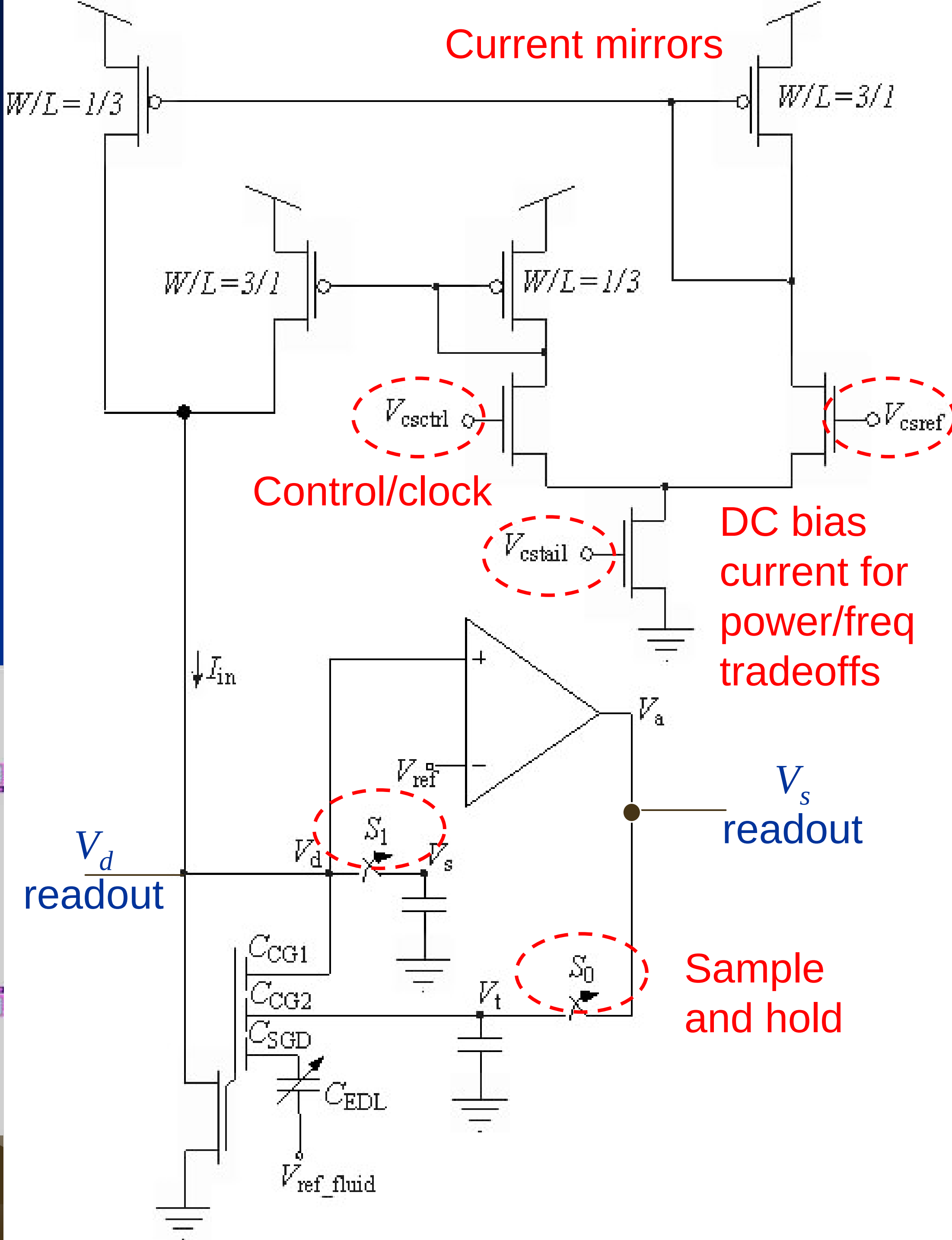

CORNELL

Sample-and-Hold Control Signal

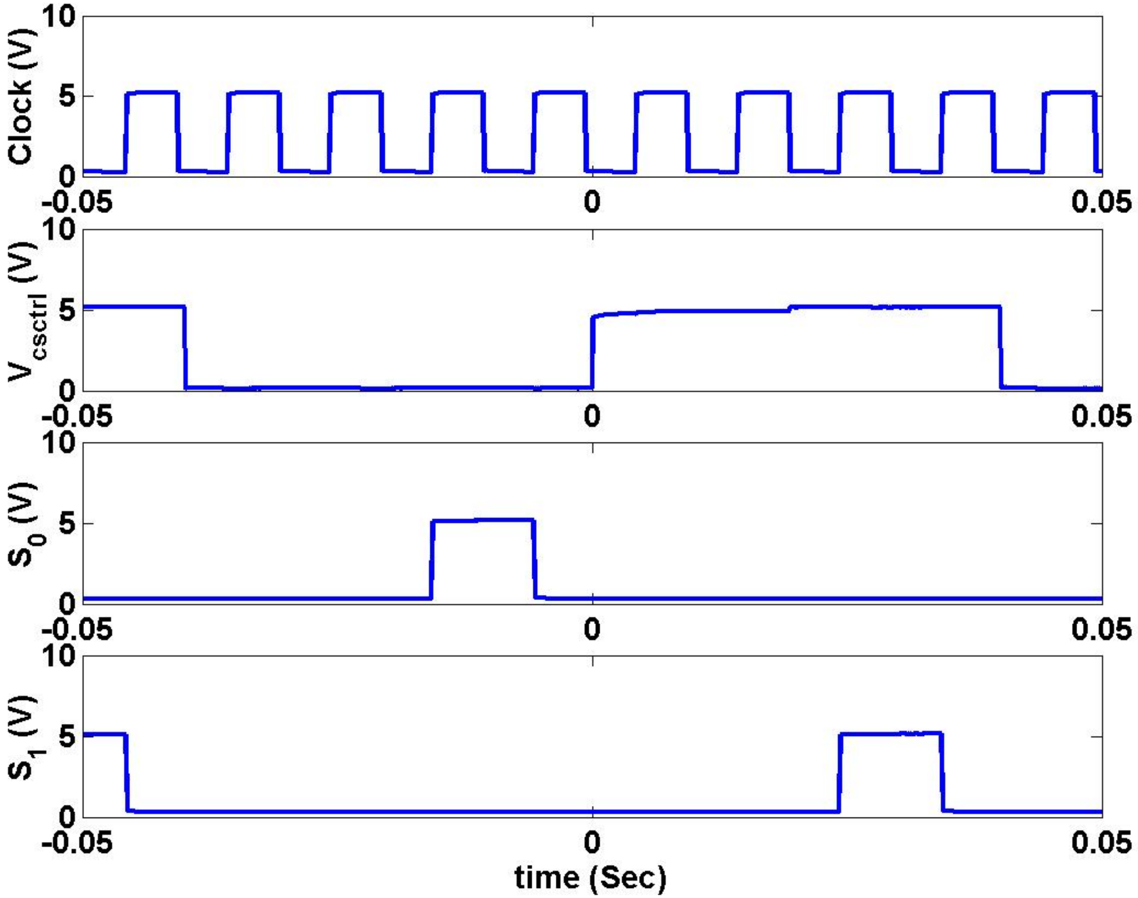

Control signal for sample and hold in the readout circuits (monitoring signals from measurement)

CORNELL

Readout Calibration

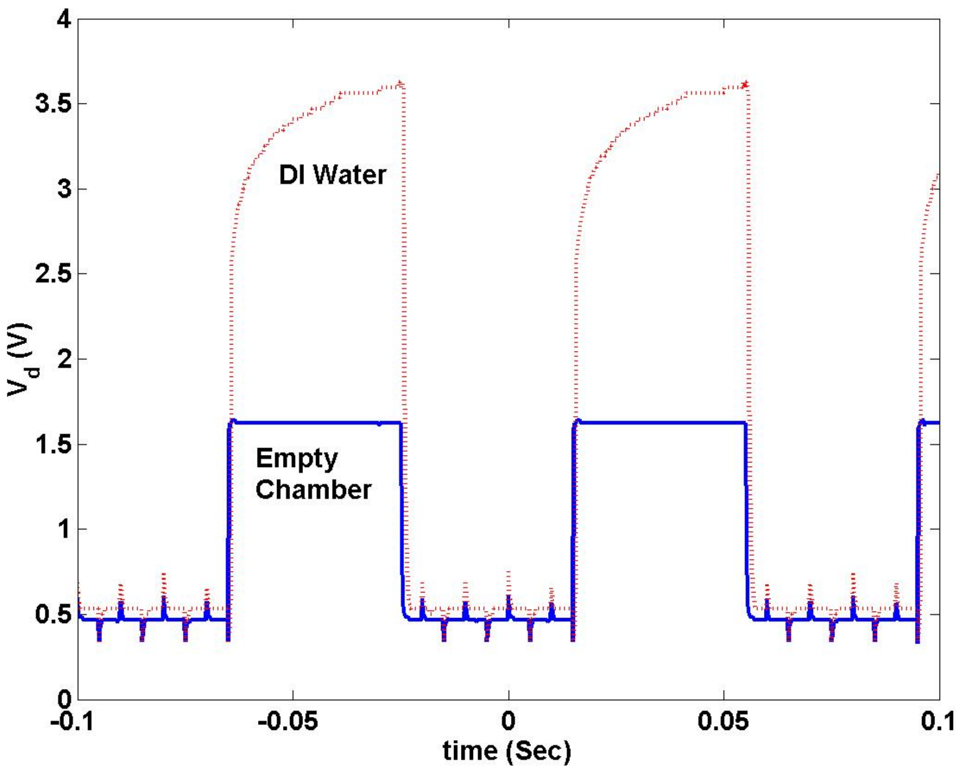

Quasi-static operations with reliable resets

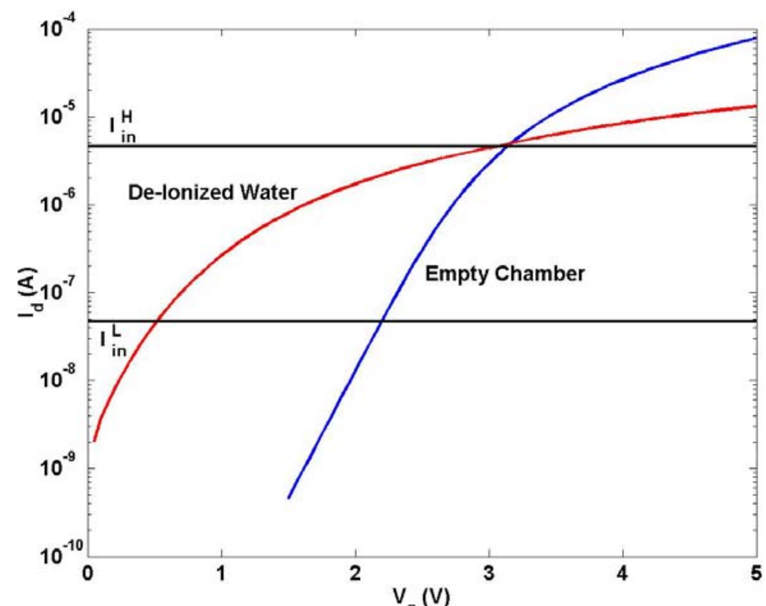

Readout Channel

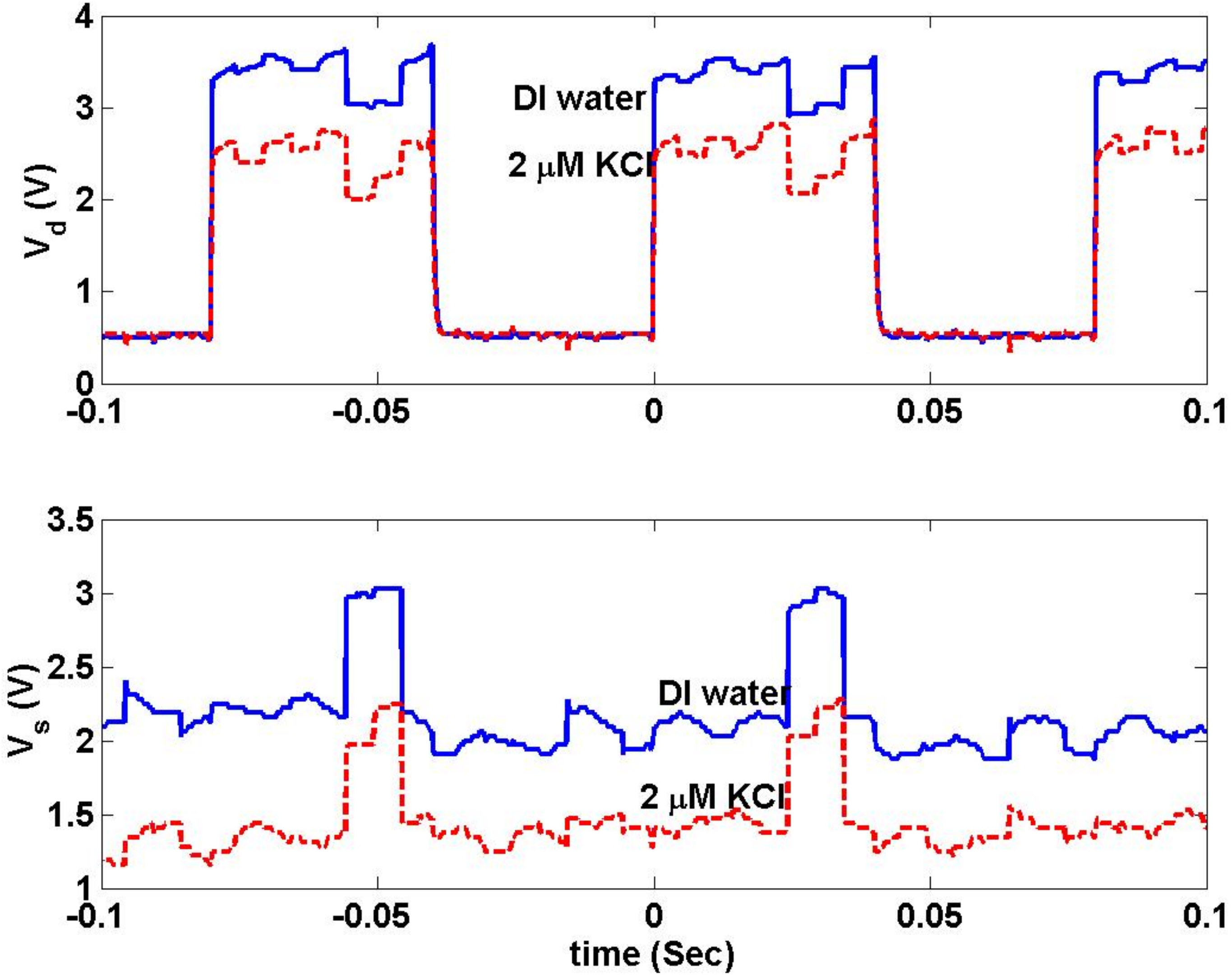

Outline

- Development of the chemoreceptive neuron MOS (CνMOS) trasistors
  - **<u>Device operations and results</u>**
    - Sensors
    - **<u>Actuators</u>**

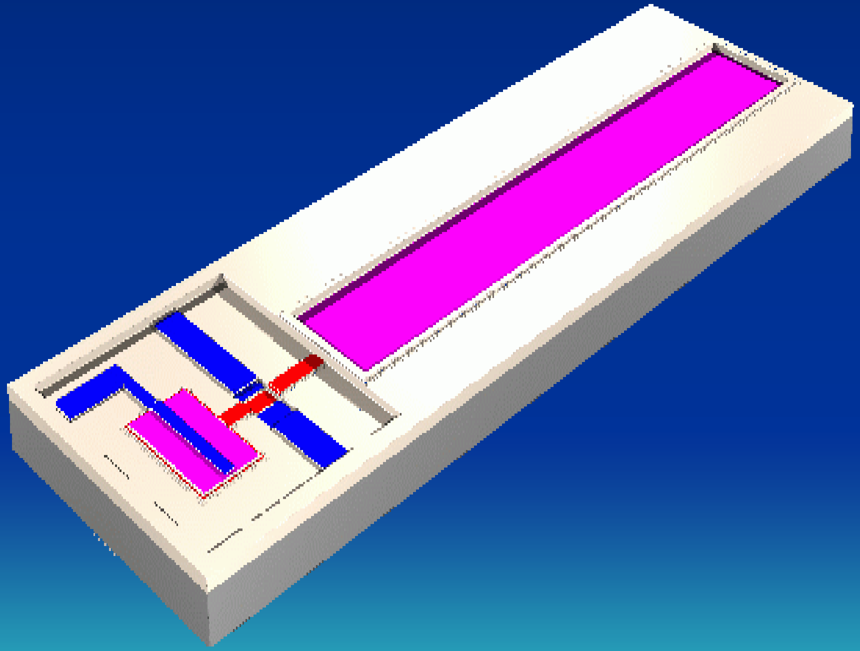

Electrowetting Actuation

- Conventional approach – the change of surface tension at the solid-liquid interface by directly applying different voltages
- Young's equation

$$\gamma_{sg} = \gamma_{s\ell} + \gamma_{\ell g}\cos\theta$$

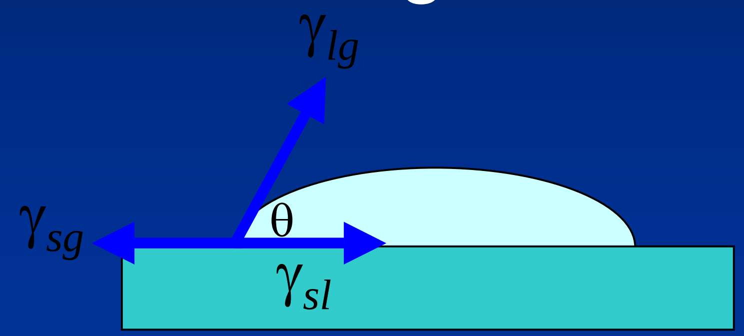

- Lippman's equation

$$\gamma_{sl} = \gamma_{sl0} - \frac{C_{edl}}{2}(V - V_0)^2$$

$$\theta = \arccos\left(\cos\theta_0 + \frac{C_{edl}}{2\gamma_{lg}}(V - V_0)^2\right)$$

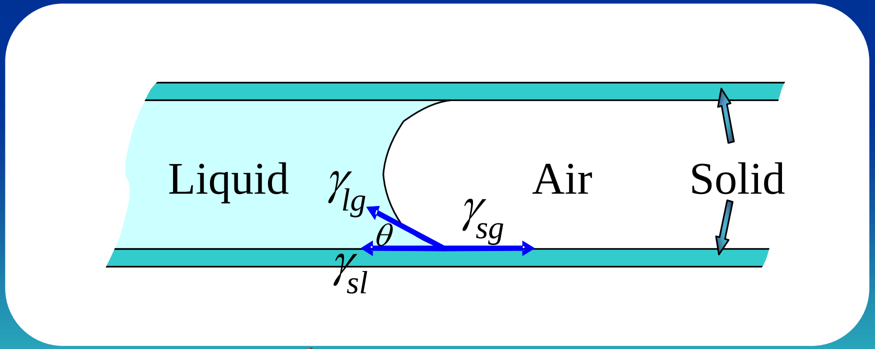

CORNELL

Device Structures

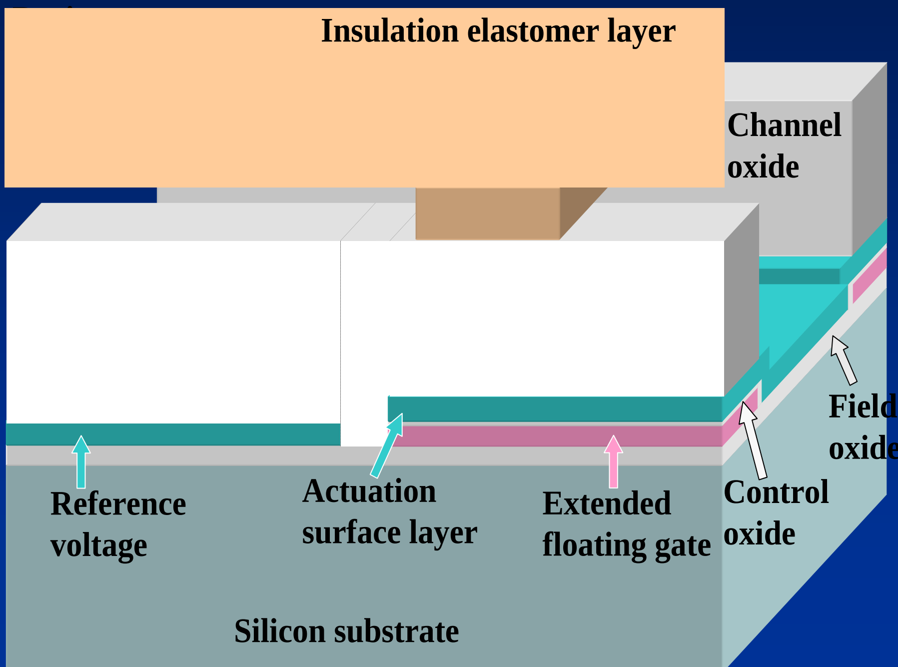

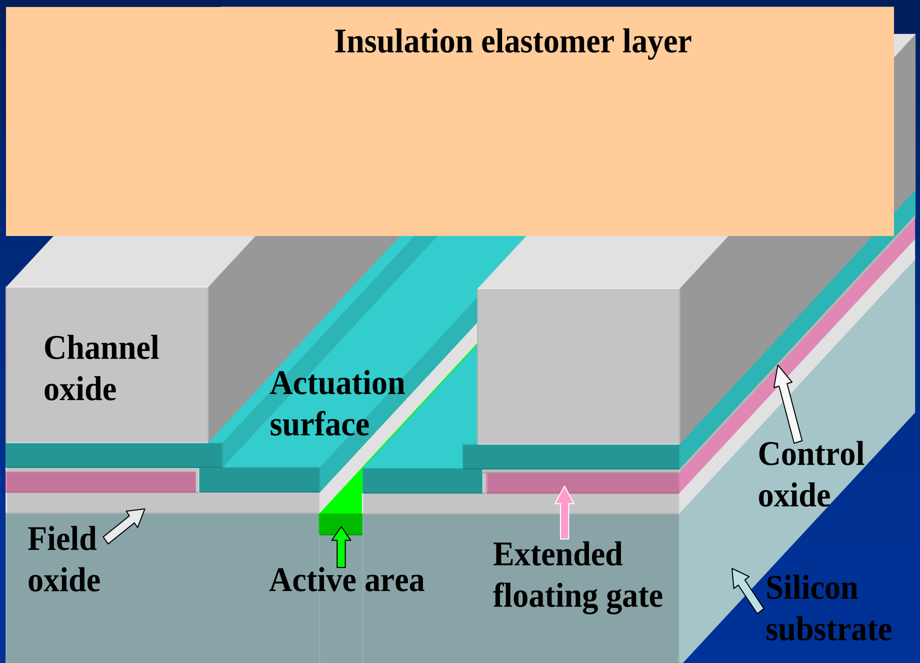

Microfluidic channel only partially covered to avoid air pressure against actuation

Transparent elastomer layer provides easy observation of the saline-water actuation

Equilibrium in the Channel

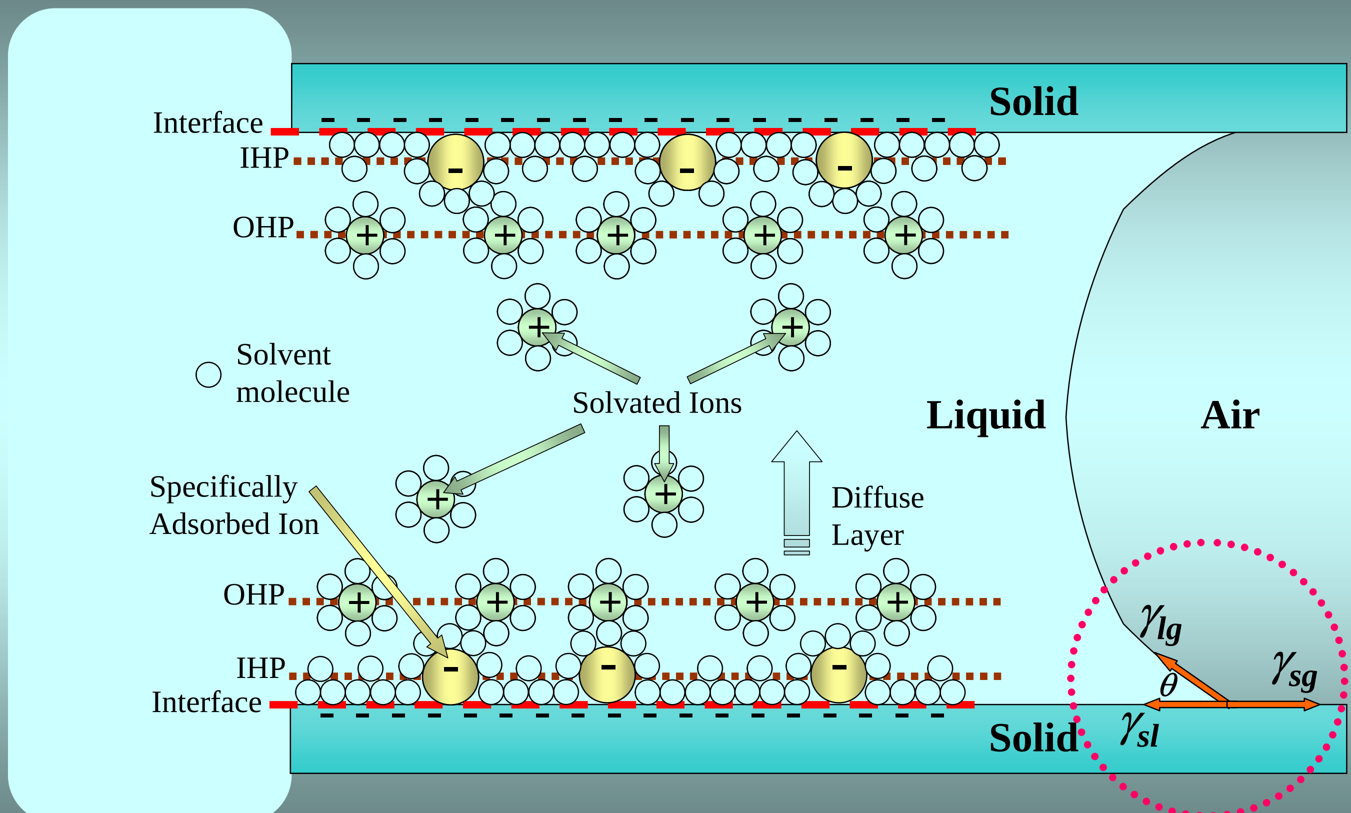

CORNELL

Actuation Scheme

Result Illustrations

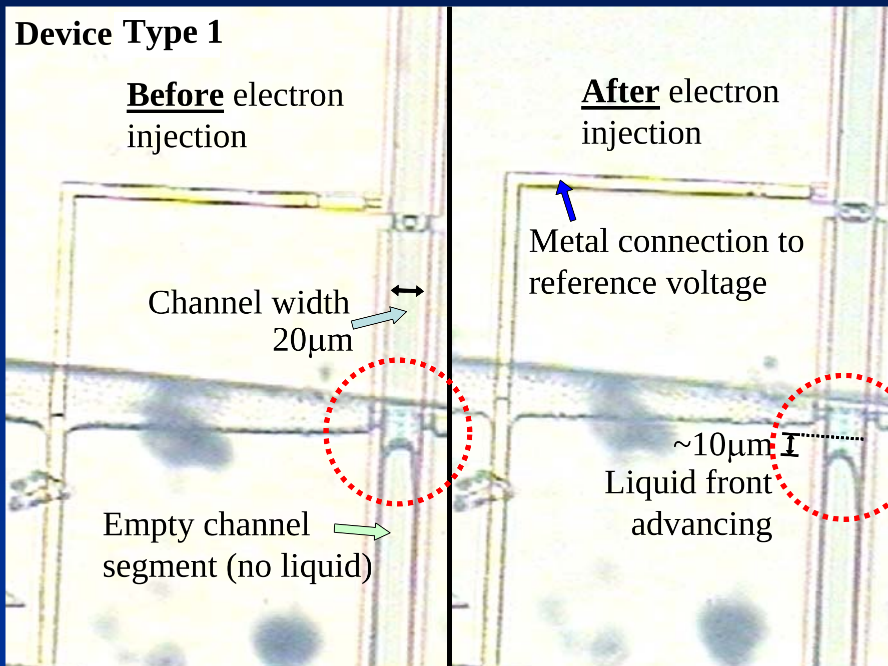

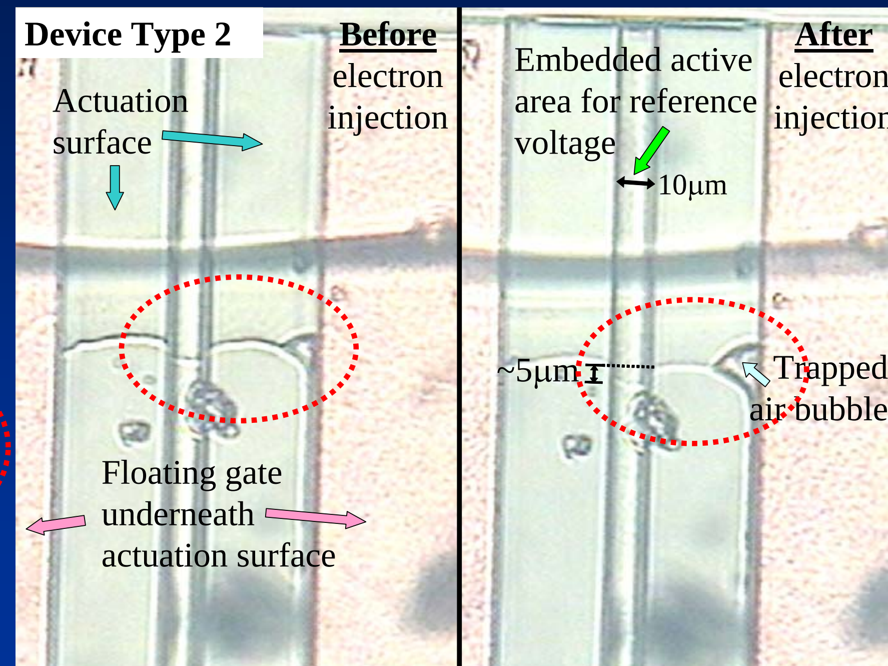

Liquid front advances about 10 μm after electrons are tunneled to the floating gate

Less change in equilibrium liquid length for the wider channel after actuation

CORNELL

Control Experiments

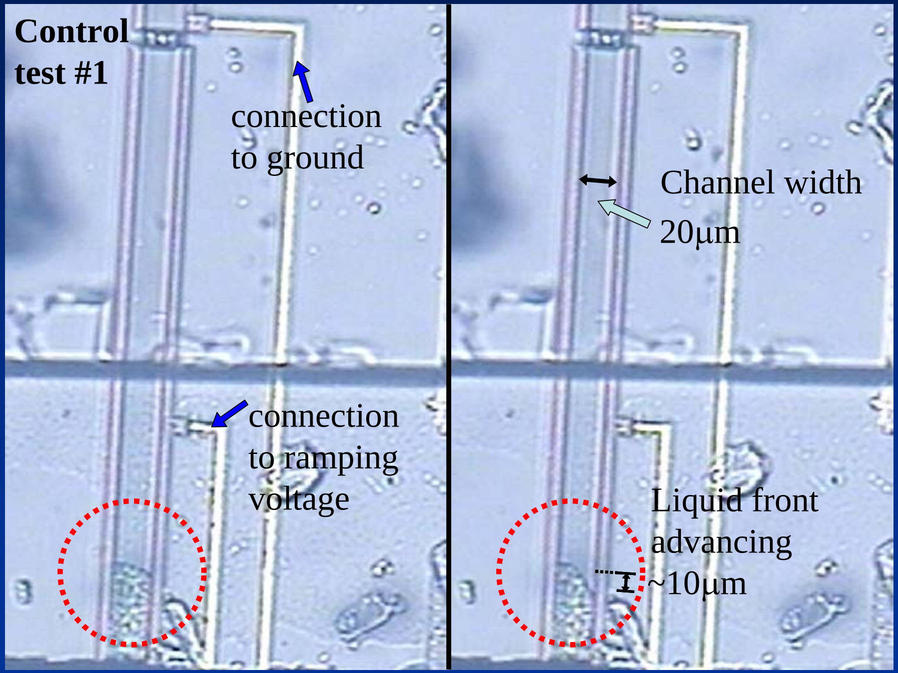

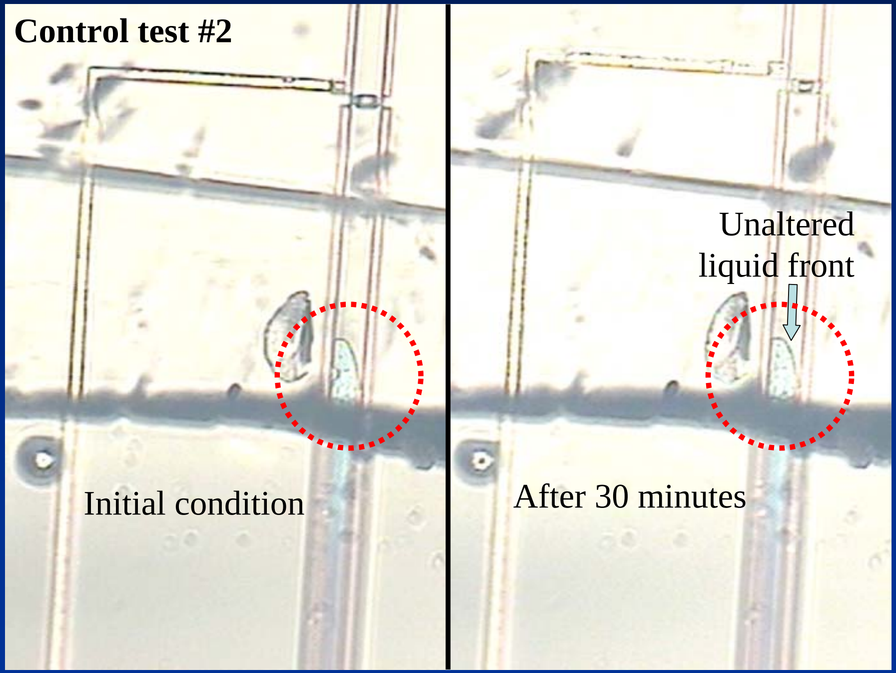

Asymmetrical liquid-front advancing by directly sweeping external voltages

Equilibrium length of the liquid almost unchanged after 30 minutes

Electrowetting on CνMOS

- Modification of interfacial charges results in the change in solid-liquid interfacial tension and hence the <u>equilibrium length</u> of the liquid in the microfluidic channel
- Potential for <u>integration</u> with the CνMOS sensors and conventional CMOS circuitry for <u>fluid delivery</u>
- Air-trapping considerations for further device designs in microfluidic application
- No actuation observed for KCl solution; results agree with $\Delta\phi_{OHP}$ after elec. injection

CORNELL

Selective to Buffer Species

- $\Delta\phi_{OHP}$ (after electron injection)

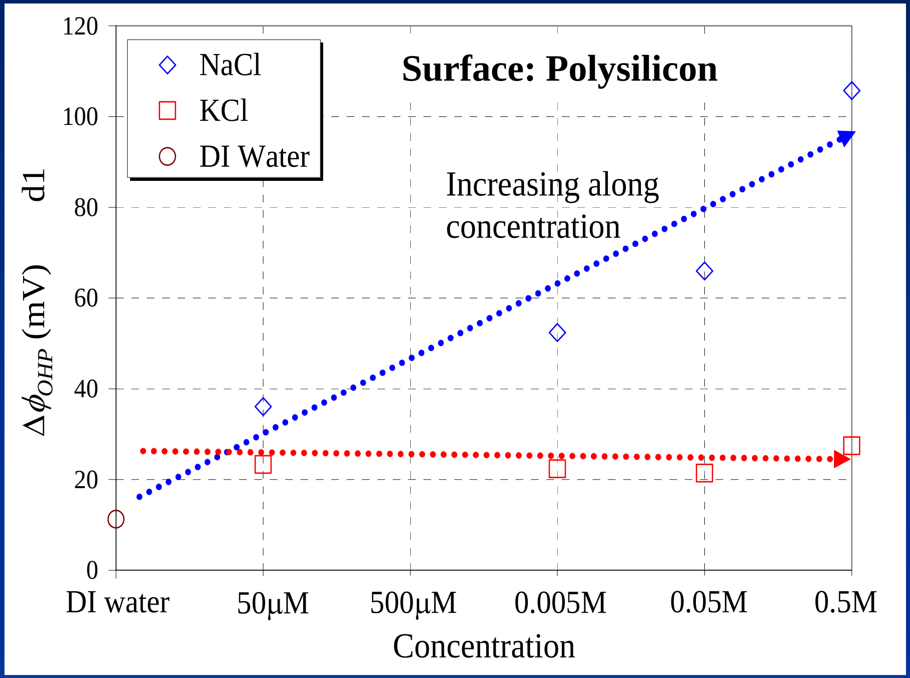

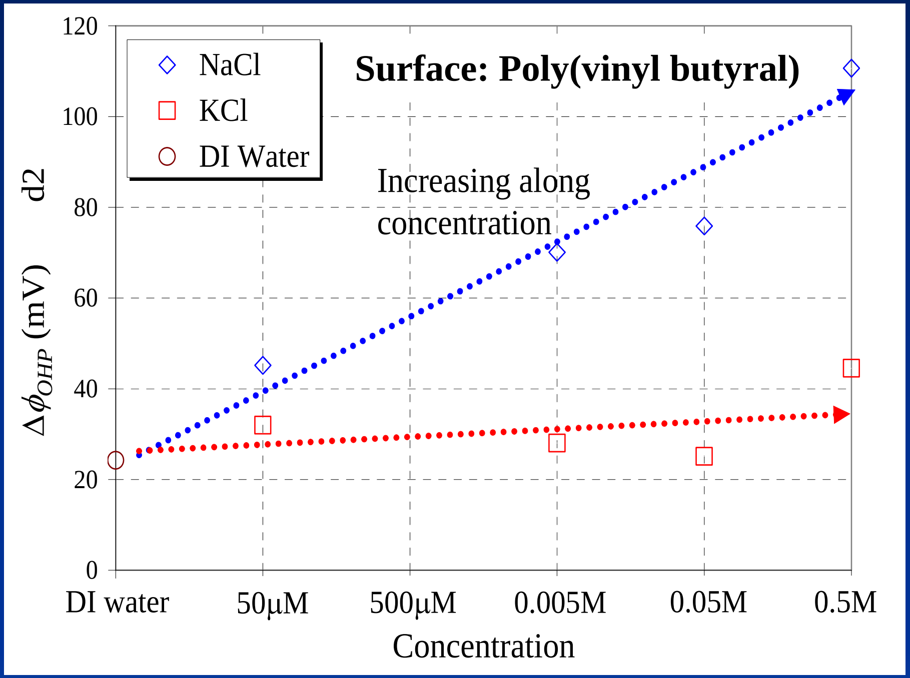

The change of the ϕ_{OHP} increases with increasing concentration in NaCl

For KCl solution, no significant increasing trend is observed as in NaCl

CORNELL

Smart Sensors and Actuators

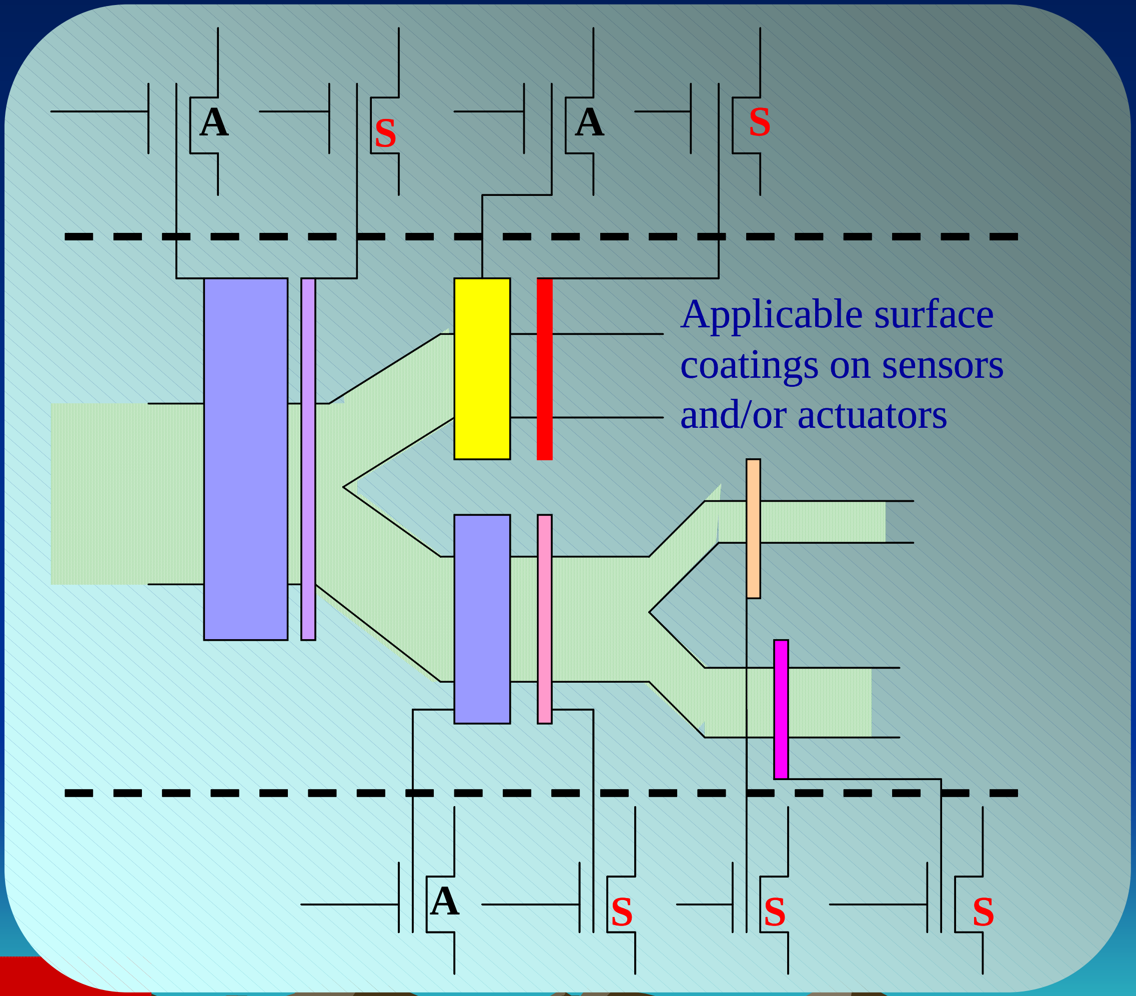

- Controlled fluid delivery for more reliable sensing
- Analysis/feedback circuitry from CMOS to provide fluid information (variety, position, etc.)
- Various surface coatings individually applied on sensors and/or actuators

Outline

- Development of the chemoreceptive neuron MOS (CνMOS) trasistors
  - Why – Review of literature
  - What – CνMOS device structure
  - How – Device operation
    - Sensors
    - Actuators

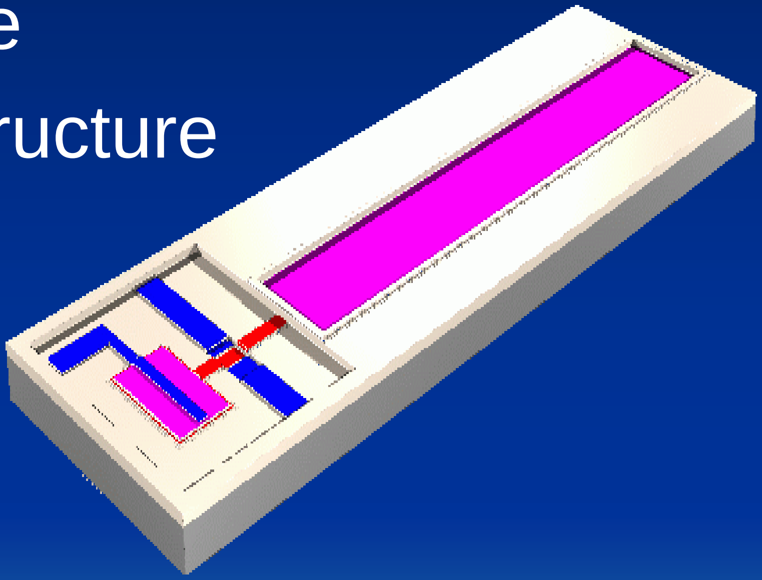

- **Summary and future directions**

Summary (1/2)

- FET devices with extended floating gates for chemical sensing
- Floating-gate structure for electron-tunneling operations provides more DOFs for sensing
- Indicators from *I-V* characteristics: Subthreshold slopes (*S*) and threshold voltages (V_t)
- CMOS integration enables detailed control circuits

CORNELL

Summary (2/2)

- Normalized ΔC_{SG} in the polymeric responses directly couples to subthreshold slopes and the patterns encourage sensor-array application in the lock-and-key implementation
- Electrowetting actuator for potential microvalves integrated with the sensors and conventional CMOS circuitry for fluid delivery and confinement

CORNELL